THE UNIVERSITY OF MANITOBA

A RAMAN LINEWIDTH INVESTIGATION OF MOLECULAR MOTION IN LIQUID BENZENE

by

Murray Norman Neuman

A THESIS

SUBMITTED TO THE FACULTY OF GRADUATE STUDIES

IN PARTIAL FULFILMENT OF THE REQUIREMENTS FOR THE DEGREE

OF MASTER OF SCIENCE

DEPARTMENT OF PHYSICS

WINNIPEG, MANITOBA

September, 1975

A RAMAN LINEWIDTH INVESTIGATION OF MOLECULAR MOTION IN LIQUID BENZENE

by

MURRAY NORMAN NEUMAN

A dissertation submitted to the Faculty of Graduate Studies of the University of Manitoba in partial fulfillment of the requirements of the degree of

MASTER OF SCIENCE

ACKNOWLEDGEMENT

The author acknowledges gratitude to his supervisor, Dr. G. C. Tabisz, for his patient guidance, and for imparting the philosophy that dragons need not be slain, but muzzled.

ABSTRACT

The reorientational and vibrational broadening of the 992 $cm.^{-1}$ A_{1g} Raman line of benzene has been investigated through linewidth analysis, in pure liquid benzene and in benzene-carbon tetrachloride liquid mixtures, over a range of temperatures. The results have been interpreted in terms of the molecular dynamics of the liquids studied.

It is concluded that tumbling motions of the benzene molecule are well described by a rotational diffusion model in the neat liquid, but appear to approach free rotor behaviour in the mixtures. Also, evidence has been found to suggest that an unusual, vibration-to-vibration energy transfer occurring during C_6H_6-C_6H_6 collisions, dominates vibrational relaxation in pure liquid benzene.

Linewidth analysis techniques that were developed in the course of this work, are discussed.

CONTENTS

LIST OF FIGURES

LIST OF TABLES

CHAPTER 1

INTRODUCTION

Experiments involving absorption or scattering of radiation can contribute many insights to the study of molecular motion in fluids, particularly in regard to intermolecular forces and the dynamics of molecular collisions. The traditional sources of information about molecular forces, such as viscosity and virial coefficients, are largely insensitive to the angular dependence or "shape" of these forces. In contrast, certain spectroscopic effects occur because of, or are modified by, the presence of intermolecular torques. For this reason, spectroscopic methods are of value in investigating the nonspherical shape of intermolecular forces. Among these methods rank microwave, infrared, and magnetic resonance absorption; also, Rayleigh, Raman, and fluorescent light scattering.

Scattering experiments enjoy a peculiar advantage over absorption experiments probing comparable molecular energy levels. If incident radiation of a definite polarisation is used, the scattering process may preserve some of the directional information encoded in the incident electric field. If the scattered radiation is analyzed according to polarisation, the spectral profile will generally depend on the polarisation mode selected. Extra information about molecular interactions can be gleaned from this polarisation dependence. That this should be so, can be made intuitively plausible. One might consider a scattering molecule which, from the point of view of incident radiation, has spherical symmetry in the absence of perturbation by neighbouring molecules. (In the case of Raman scattering, for instance, the required symmetry consists in a spherical polarisability tensor.)

One might further suppose, that any environmental perturbation of the scattering molecule takes the form of intermolecular forces of spherical shape. If the experimental geometry has been arranged so that the polarisation vector of the incident radiation is normal to the scattering plane, then, by an elementary symmetry argument, the scattering process cannot be expected to change the direction of the polarisation vector. Any such change which is actually observed, must therefore be a manifestation of asphericity, either in the structure of the molecule or in the forces coupling it to its environment. Thus, when scattering molecules are selected, which are known to possess certain symmetry elements, a clear connection can sometimes be drawn between the depolarisation of the scattered radiation and the angular dependence of the intermolecular forces.

When applied to the analysis of Raman vibrational lines of certain symmetry species, the polarisation dependence of the scattering spectrum is a particularly convenient happenstance. If a few plausible assumptions are granted, it allows of a tidy separation of rotational line-broadening from that induced by other mechanisms (especially vibrational relaxation). This feature will be exploited in the course of our investigations.

In the present work, we shall examine the rotational broadening of the 992 $cm.^{-1}$ A_{1g} Raman vibrational line in liquid benzene, both as a neat liquid and in solution with CCl_4. An explicit description of the angular dependence of intermolecular forces is beyond the scope of this work, and, indeed, beyond the present state of the art. We shall, however, use lineshape parameters to derive rotational diffusion constants, which may be interpreted in terms of the degree to which,

and the manner in which, molecular reorientation is hindered by interactions with neighbouring molecules. Such hindrance would not exist if the coupling forces were spherical; the diffusion constants are thus related to the nonspherical shape of the forces. The temperature and concentration dependence of the diffusion constants may further illuminate the kinematic nature of molecular reorientation, and thence the dynamics governing it.

In addition to the study of molecular reorientation, we undertake to examine the temperature and concentration dependence of vibrational relaxation time for the Raman line in question, again by analyzing lineshapes. Insofar as vibrational relaxation occurs as a result of molecular collisions, these times are indicative of the "time between collisions", and are source of further information about the molecular dynamics of the fluid under study.

Only recently[1] have Raman and infrared lineshapes come to be regarded as a problem involving, or conversely as a clue to, the time dependence of molecular variables in a statistical ensemble. The formalism which relates lineshapes to molecular motion, is a time correlation function of the molecular variables. The use of correlation function expressions in analyzing lineshape data for liquids has now gained wide acceptance, as it has, indeed, in describing a wide range of disparate physical phenomena, particularly transport processes.[2]

References:

1. R. G. Gordon, J. Chem. Phys. 43, 1307 (1965).

2. R. Zwanzig, Ann. Rev. Phys. Chem. 16, 67 (1965).

CHAPTER 2

THEORY

In the following discussion, a quantum mechanical description of Raman light scattering will be formulated. Once the general connection between the spectral profile and the time dependence of molecular dynamic variables has been established, a framework will be constructed, within which lineshape parameters may be interpreted in terms of the motion of individual molecules.

I. Quantum Mechanical Description of Light Scattering:

Following Gordon[1], we begin with the polarisability formula developed by Placzek[2] for non-resonant Raman scattering. These authors give the cross section (probability per unit solid angle Ω, per unit angular frequency ω, that an incident photon will be scattered into $d\Omega d\omega$) as

$$\frac{d^2\sigma}{d\Omega d\omega} = \frac{\omega^{(1)}(\omega^{(2)})^3}{c^4} \sum_{if} |\langle i|\hat{\varepsilon}^{(1)}\cdot\overleftrightarrow{a}\cdot\hat{\varepsilon}^{(2)}|f\rangle|^2 \rho_i \delta(\omega_{fi}-\omega) \qquad \ldots (2.1)$$

Here, $\omega = \omega^{(1)} - \omega^{(2)}$, where $\omega^{(1)}$ and $\omega^{(2)}$ are the angular frequencies of the incident and scattered photons, respectively; $\hat{\varepsilon}^{(1)}$ and $\hat{\varepsilon}^{(2)}$ are unit vectors along the directions of the electric vectors of the incident and scattered photons, respectively; $|i\rangle$ and $|f\rangle$ range over the (many-particle) eigenfunctions of the scattering system, and have energy eigenvalues E_i and E_f; ω_{fi} is the Bohr frequency $(E_f - E_i)/\hbar$; ρ_i is the probability of finding the scattering system initially in state $|i\rangle$; $\overleftrightarrow{a}$ is the polarisability tensor of the scattering system, evaluated in the lab frame.

(NOTE: Equation (2.1) differs by the factor $\omega^{(1)}/\omega^{(2)}$ from the form given in References 1. and 2., because these authors measure radiation fluxes

in terms of energy, rather than number of photons.)

This formula represents the conventional Schrödinger picture of Raman spectroscopy, in that it focuses attention on the energy levels, rather than the time development, of the system. It has little interpretive value, for, since there is no classical analogue of a single quantum state, it does not allow any classical correspondence to be exploited. The Heisenberg picture, on the other hand, leads naturally to the expression of a spectrum as the Fourier transform of a time correlation function, and yields the classical result in the appropriate limit.

In order to proceed from (2.1) to the corresponding Heisenberg form, one introduces the Fourier representation of the Dirac δ function:

$$\delta(\omega) = (2\pi)^{-1}\int_{-\infty}^{\infty} dt\ \exp(i\omega t) \quad , \qquad \text{whence}$$

$$\frac{d^2\sigma}{d\Omega d\omega} = \frac{\omega^{(1)}(\omega^{(2)})^3}{2\pi c^4}\sum_{if}\rho_i\langle i|\hat{\varepsilon}^{(1)}\cdot\overleftrightarrow{a}\cdot\hat{\varepsilon}^{(2)}|f\rangle\langle f|\hat{\varepsilon}^{(1)}\cdot\overleftrightarrow{a}\cdot\hat{\varepsilon}^{(2)}|i\rangle\int_{-\infty}^{\infty}dt\ \exp i\left[\frac{E_f-E_i}{\hbar}-\omega\right]t$$

$$= \frac{\omega^{(1)}(\omega^{(2)})^3}{2\pi c^4}\int_{-\infty}^{\infty}dt\ \exp(-i\omega t)\sum_{if}\rho_i\langle i|(\hat{\varepsilon}^{(1)}\cdot\overleftrightarrow{a}\cdot\hat{\varepsilon}^{(2)})\exp(iE_f t/\hbar)|f\rangle$$

$$\times\langle f|(\hat{\varepsilon}^{(1)}\cdot\overleftrightarrow{a}\cdot\hat{\varepsilon}^{(2)})\exp(-iE_i t/\hbar)|i\rangle \ ,$$

where, in the last step, the multipliers $\exp(iE_f t/\hbar)$ and $\exp(-iE_i t/\hbar)$ have been taken inside the scalar products, and the linearity of the operator $\hat{\varepsilon}^{(1)}\cdot\overleftrightarrow{a}\cdot\hat{\varepsilon}^{(2)}$ has been used. This result may be re-expressed by introducing the Hamiltonian H of the matter (excluding the interaction of the radiation and matter). Since $|i\rangle$ and $|f\rangle$ are eigenstates of H with eigenvalues E_i and E_f , one may write[3]

$$\exp(iE_f t/\hbar)|f\rangle = \exp(iHt/\hbar)|f\rangle \qquad \text{and}$$

$$\exp(-iE_i t/\hbar)|i\rangle = \exp(-iHt/\hbar)|i\rangle\,, \qquad \text{whence}$$

$$\frac{d^2\sigma}{d\Omega d\omega} = \frac{\omega^{(1)}(\omega^{(2)})^3}{2\pi c^4}\int_{-\infty}^{\infty} dt\, \exp(-i\omega t)\sum_{if} \rho_i \langle i|(\hat{\varepsilon}^{(1)}\cdot\overleftrightarrow{a}\cdot\hat{\varepsilon}^{(2)})\exp(iHt/\hbar)|f\rangle$$

$$\times\langle f|(\hat{\varepsilon}^{(1)}\cdot\overleftrightarrow{a}\cdot\hat{\varepsilon}^{(2)})\exp(-iHt/\hbar)|i\rangle.$$

One may invoke the completeness relation

$$\sum_f |f\rangle\langle f| = 1$$

to remove the sum over final states:

$$\frac{d^2\sigma}{d\Omega d\omega} = \frac{\omega^{(1)}(\omega^{(2)})^3}{2\pi c^4}\int_{-\infty}^{\infty} dt\, \exp(-i\omega t)\sum_i \rho_i \langle i|[\hat{\varepsilon}^{(1)}\cdot\overleftrightarrow{a}\cdot\hat{\varepsilon}^{(2)}]$$

$$\times[\exp(iHt/\hbar)(\hat{\varepsilon}^{(1)}\cdot\overleftrightarrow{a}\cdot\hat{\varepsilon}^{(2)})\exp(-iHt/\hbar)]|i\rangle.$$

The second square bracket within the scalar product may be recognized[4] as the time - dependent operator $\hat{\varepsilon}^{(1)}\cdot\overleftrightarrow{a}\cdot\hat{\varepsilon}^{(2)}$, evaluated at time t, and may be written as $\hat{\varepsilon}^{(1)}\cdot\overleftrightarrow{a}(t)\cdot\hat{\varepsilon}^{(2)}$, since $\hat{\varepsilon}^{(1)}$ and $\hat{\varepsilon}^{(2)}$ are constant in time. The first square bracket may likewise be recognized as the same operator at time 0, and written as $\hat{\varepsilon}^{(1)}\cdot\overleftrightarrow{a}(0)\cdot\hat{\varepsilon}^{(2)}$. Thus,

$$\frac{d^2\sigma}{d\Omega d\omega} = \frac{\omega^{(1)}(\omega^{(2)})^3}{2\pi c^4}\int_{-\infty}^{\infty} dt\, \exp(-i\omega t)\sum_i \rho_i \langle i|[\hat{\varepsilon}^{(1)}\cdot\overleftrightarrow{a}(0)\cdot\hat{\varepsilon}^{(2)}][\hat{\varepsilon}^{(1)}\cdot\overleftrightarrow{a}(t)\cdot\hat{\varepsilon}^{(2)}]|i\rangle.$$

The weighted sum over expectation values corresponding to the various initial states, constitutes a quantum statistical average, which we denote by $\langle\ \rangle_0$:

$$\frac{d^2\sigma}{d\Omega d\omega} = \frac{\omega^{(1)}(\omega^{(2)})^3}{2\pi c^4}\int_{-\infty}^{\infty} dt\, \exp(-i\omega t)\langle[\hat{\varepsilon}^{(1)}\cdot\overleftrightarrow{a}(0)\cdot\hat{\varepsilon}^{(2)}][\hat{\varepsilon}^{(1)}\cdot\overleftrightarrow{a}(t)\cdot\hat{\varepsilon}^{(2)}]\rangle_0 \quad \ldots \quad (2.2)$$

If the average $\langle\,\rangle_0$ is interpreted as a classical ensemble average, one recovers the classical description[5] of Raman scattering, as the Fourier transform of a time correlation function.

II. Reduction of Polarisability to that of Single Molecule:

In (2.2), the polarisability tensor $\overleftrightarrow{\alpha}$ pertains to a whole group of interacting molecules exposed to the incident radiation, and consists, we assume, in the sum of the polarisabilities of the individual molecules. Thus, every product of $\overleftrightarrow{\alpha}(0)$ and $\overleftrightarrow{\alpha}(t)$ will contain cross terms between the polarisabilities of different molecules. If it is assumed that there are no angular correlations among the orientations of neighbouring molecules, then the ensemble averages of these cross terms will vanish, and the correlation function in (2.2) will equal N times the single-molecule correlation function, where N is the number of molecules contributing to the scattering. When we take cognizance of this cancellation of cross terms, (2.2) stands as written above, but $\frac{d^2\sigma}{d\Omega d\omega}$ will now be interpreted as the cross section per scattering molecule, and the polarisability tensor $\overleftrightarrow{\alpha}$ as that of a single molecule. The reduction we have just effected, is central to our objective of describing the scattering spectrum in terms of the motion of a single molecule.

Felicitous though it may be to neglect angular correlations, the assumption involved should be applied only with strict reservations. The evident existence of hindered rotations in liquids must be due to intermolecular torques, whose presence implies that the potential energy of interacting molecules is a function of their relative orientations. As a result, some relative orientations will be more energetically favourable than others, and a degree of angular correlation

is inevitable. Quantitative calculations of such effects are difficult to find in the literature, so that no satisfactory treatment can be given here.

One may proceed further to evaluate the expression within the ensemble average of (2.2). It is assumed that the scattering system is isotropic - i.e., that the molecule - fixed axes are randomly oriented with respect to the polarisation vectors $\hat{\mathcal{E}}^{(1)}$ and $\hat{\mathcal{E}}^{(2)}$ - as will, indeed, be the case for a liquid or gas sample. The ensemble average of (2.2) may be performed by averaging independently over molecular orientations and over molecular eigenstates. The separation of the two averages is justified by the fact, that the eigenstates are indifferent to the orientation of the molecule in the lab frame. They could depend on orientation only through the interaction of the matter with the incident radiation, and we have postulated in I. that this interaction may be excluded from the Hamiltonian which determines the eigenstates.

Assuming isotropy of the scattering system, we shall first average explicitly over molecular orientations. Letting $I_{\parallel}$ and $I_{\perp}$ * denote the cross sections when $\hat{\mathcal{E}}^{(1)}$ and $\hat{\mathcal{E}}^{(2)}$ are, respectively, parallel and perpendicular to each other, one obtains[6] from (2.2):

$$I_{\parallel}(\omega) = \frac{\omega^{(1)}(\omega^{(2)})^3}{2\pi c^4}\int_{-\infty}^{\infty} dt\, \exp(-i\omega t)\left\langle \frac{1}{15}\sum_{jk}\left[2a_{jk}(0)a_{jk}(t) + a_{jj}(0)a_{kk}(t)\right]\right\rangle$$

and $$I_{\perp}(\omega) = \frac{\omega^{(1)}(\omega^{(2)})^3}{2\pi c^4}\int_{-\infty}^{\infty} dt\, \exp(-i\omega t)\left\langle \frac{1}{30}\sum_{jk}\left[3a_{jk}(0)a_{jk}(t) - a_{jj}(0)a_{kk}(t)\right]\right\rangle,$$

where $\langle\,\rangle$ now denotes the usual thermal (Boltzmann) average.

Next, one may separate $\overleftrightarrow{a}$ into its anisotropic (traceless) and spherical parts:

---

* $I_{\parallel}$ and $I_{\perp}$ will subsequently be referred to as the "polarised" and "depolarised" spectra, respectively.

$$a_{ij} = \bar{\alpha}\,\delta_{ij} + \beta_{ij} \quad , \text{ where } \quad \bar{\alpha} = \tfrac{1}{3}\,\mathrm{Tr}(\overleftrightarrow{a}) \; .$$

Writing the summations over j and k in trace (Tr) notation, one readily gets [6]

$$I_{\parallel}(\omega) = \frac{\omega^{(1)}(\omega^{(2)})^3}{2\pi c^4} \int_{-\infty}^{\infty} dt \, \exp(-i\omega t) \left\langle \bar{\alpha}(0)\bar{\alpha}(t) + \tfrac{2}{15}\,\mathrm{Tr}\left[\overleftrightarrow{\beta}(0)\cdot\overleftrightarrow{\beta}(t)\right] \right\rangle \quad \ldots \text{ (2.3a)}$$

and

$$I_{\perp}(\omega) = \frac{\omega^{(1)}(\omega^{(2)})^3}{2\pi c^4} \int_{-\infty}^{\infty} dt \, \exp(-i\omega t) \left\langle \tfrac{1}{10}\,\mathrm{Tr}\left[\overleftrightarrow{\beta}(0)\cdot\overleftrightarrow{\beta}(t)\right] \right\rangle . \quad \ldots \text{ (2.3b)}$$

It is convenient to define the isotropic or "trace" scattering by

$$I_{iso}(\omega) = \frac{\omega^{(1)}(\omega^{(2)})^3}{2\pi c^4} \int_{-\infty}^{\infty} dt \, \exp(-i\omega t) \left\langle \bar{\alpha}(0)\bar{\alpha}(t) \right\rangle , \quad \ldots \text{ (2.4a)}$$

and the anisotropic scattering by

$$I_{anis}(\omega) = \frac{\omega^{(1)}(\omega^{(2)})^3}{2\pi c^4} \int_{-\infty}^{\infty} dt \, \exp(-i\omega t) \left\langle \tfrac{1}{10}\,\mathrm{Tr}\left[\overleftrightarrow{\beta}(0)\cdot\overleftrightarrow{\beta}(t)\right] \right\rangle \quad \ldots \text{ (2.4b)}$$

It is evidently possible, experimentally to separate the anisotropic from the trace scattering: from (2.3), we see that

$$I_{anis}(\omega) = I_{\perp}(\omega) \quad \ldots \text{ (2.5a)}$$

and

$$I_{iso}(\omega) = I_{\parallel}(\omega) - \tfrac{4}{3}\, I_{\perp}(\omega) \; . \quad \ldots \text{ (2.5b)}$$

III. <u>Separation of Reorientational and Vibrational Broadening Mechanisms:</u>

We shall now investigate the form taken by (2.4), when a vibrational Raman spectrum is considered, and when certain assumptions are adopted in regard to correlations among motions in the various degrees of

freedom of the scattering molecule.

In Gordon's original treatment[1], it was postulated that the polarisability tensor $\overleftrightarrow{\alpha}$ is constant in time, if referred to a co-ordinate system which rotates with the molecule. The time dependence of $\overleftrightarrow{\alpha}$, as evaluated in the lab frame, was thus taken to arise solely through molecular reorientation, with the result that other line-broadening mechanisms were neglected. More recent authors[6,7] have taken explicit account of vibrational broadening.

Following Bartoli and Litovitz[7], we shall consider the polarisability tensor $\overleftrightarrow{\alpha}$ to be modulated by each of the Raman-active normal vibrations of the molecule. These vibrations are assumed harmonic. A Taylor series expansion of α_{jk}, in powers of the normal co-ordinates $q^{\mu}(t)$, yields, to first order,

$$\alpha_{jk}(t) = \alpha^{o}_{jk}(t) + \sum_{\mu} \alpha^{\mu}_{jk}(t)\, q^{\mu}(t) \ ,$$

where $\alpha^{o}_{jk}(t)$ is the equilibrium ($q^{\mu}=0$) polarisability, and where

$$\alpha^{\mu}_{jk}(t) \equiv \partial \alpha_{jk}(t) / \partial q^{\mu}(t) \Big|_{q^{\mu}=0} \ .$$

Here, α^{o}_{jk} and α^{μ}_{jk} are taken to be constant when referred to the molecular axes, so that their time dependence in the lab frame arises solely through molecular reorientation. In principle, other processes, such as collisions, may contribute to the time dependence, so that the following treatment represents only a limited generalization of Gordon's approach.

Upon decomposing $\overleftrightarrow{\alpha}$ into its spherical and traceless parts, we further break down $\bar{\alpha}(t)$ and $\beta_{jk}(t)$ in the manner of $\alpha_{jk}(t)$ above.

The thermal averages occurring in (2.4) may then be re-expressed:

$$\left\langle \mathrm{Tr}\left[\overleftrightarrow{\beta}(0)\cdot\overleftrightarrow{\beta}(t)\right]\right\rangle$$

$$= \sum_{ij} \left\langle \beta_{ij}(0)\beta_{ij}(t)\right\rangle$$

$$= \sum_{ij}\Big[\left\langle \beta^{\circ}_{ij}(0)\beta^{\circ}_{ij}(t)\right\rangle + \sum_{\mu}\left\langle \beta^{\circ}_{ij}(0)\beta^{\mu}_{ij}(t)q^{\mu}(t)\right\rangle$$

$$+ \sum_{\mu}\left\langle \beta^{\circ}_{ij}(t)\beta^{\mu}_{ij}(0)q^{\mu}(0)\right\rangle + \sum_{\mu\nu}\left\langle \beta^{\mu}_{ij}(0)\beta^{\nu}_{ij}(t)q^{\mu}(0)q^{\nu}(t)\right\rangle\Big] \ldots \quad (2.6)$$

Some simplification occurs, if it is assumed that the q^{μ} are not coupled to the orientation of the molecule, and that the normal modes may be treated as independent oscillators. Now, if q^{μ} is uncorrelated with orientation, and hence with β°_{ij} and β^{μ}_{ij} (which depend only on orientation), then

$$\left\langle \beta^{\circ}_{ij}(0)\,\beta^{\mu}_{ij}(t)\,q^{\mu}(t)\right\rangle = \left\langle \beta^{\circ}_{ij}(0)\,\beta^{\mu}_{ij}(t)\right\rangle\left\langle q^{\mu}(t)\right\rangle .$$

For a harmonic oscillator, $\left\langle q^{\mu}(t)\right\rangle = 0$.

$$\therefore \left\langle \beta^{\circ}_{ij}(0)\,\beta^{\mu}_{ij}(t)\,q^{\mu}(t)\right\rangle = 0, \qquad \ldots (2.7a)$$

and similarly $\left\langle \beta^{\circ}_{ij}(t)\,\beta^{\mu}_{ij}(0)\,q^{\mu}(0)\right\rangle = 0$. $\qquad \ldots (2.7b)$

Moreover, if q^{μ} is uncorrelated with orientation, then

$$\left\langle \beta^{\mu}_{ij}(0)\,\beta^{\nu}_{ij}(t)\,q^{\mu}(0)\,q^{\nu}(t)\right\rangle = \left\langle \beta^{\mu}_{ij}(0)\,\beta^{\nu}_{ij}(t)\right\rangle\left\langle q^{\mu}(0)\,q^{\nu}(t)\right\rangle .$$

If different normal modes are independent, then

$$\langle q^{\mu}(0)\, q^{\nu}(t)\rangle = \langle q^{\mu}(0)\rangle\langle q^{\nu}(t)\rangle = 0 \quad \text{for} \quad \mu \neq \nu .$$

$$\therefore \sum_{\mu\nu}\langle \beta_{ij}^{\mu}(0)\,\beta_{ij}^{\nu}(t)\, q^{\mu}(0)\, q^{\nu}(t)\rangle = \sum_{\mu}\langle \beta_{ij}^{\mu}(0)\,\beta_{ij}^{\mu}(t)\rangle\langle q^{\mu}(0)\, q^{\mu}(t)\rangle . \qquad \ldots (2.8)$$

With the results (2.7) and (2.8), (2.6) becomes

$$\langle \mathrm{Tr}[\overleftrightarrow{\beta}(0)\cdot\overleftrightarrow{\beta}(t)]\rangle = \sum_{ij}\Big[\langle \beta_{ij}^{\circ}(0)\beta_{ij}^{\circ}(t)\rangle + \sum_{\mu}\langle \beta_{ij}^{\mu}(0)\beta_{ij}^{\mu}(t)\rangle\langle q^{\mu}(0)\, q^{\mu}(t)\rangle\Big]$$

$$= \langle \mathrm{Tr}[\overleftrightarrow{\beta}^{\circ}(0)\cdot\overleftrightarrow{\beta}^{\circ}(t)]\rangle + \sum_{\mu}\langle \mathrm{Tr}[\overleftrightarrow{\beta}^{\mu}(0)\cdot\overleftrightarrow{\beta}^{\mu}(t)]\rangle\langle q^{\mu}(0)\, q^{\mu}(t)\rangle . \qquad \ldots (2.6')$$

Treating $\overline{\alpha}$ as we have treated individual components of $\overleftrightarrow{\beta}$, we find

$$\langle \overline{\alpha}(0)\,\overline{\alpha}(t)\rangle = \langle \overline{\alpha}^{\circ}(0)\,\overline{\alpha}^{\circ}(t)\rangle + \sum_{\mu}\langle \overline{\alpha}^{\mu}(0)\,\overline{\alpha}^{\mu}(t)\rangle\langle q^{\mu}(0)\, q^{\mu}(t)\rangle .$$

Now, the time dependence of $\overline{\alpha}^{\circ}$ and $\overline{\alpha}^{\mu}$ was supposed to arise, if at all, through molecular reorientation. But $\overline{\alpha}^{\circ}$ and $\overline{\alpha}^{\mu}$ are, by definition, rotational invarients (since the trace of a matrix is invariant under rotation). Thus $\overline{\alpha}^{\circ}$ and $\overline{\alpha}^{\mu}$ are constant in time, and we may write

$$\langle \overline{\alpha}(0)\,\overline{\alpha}(t)\rangle = \langle (\overline{\alpha}^{\circ})^2\rangle + \sum_{\mu}\langle (\overline{\alpha}^{\mu})^2\rangle\langle q^{\mu}(0)\, q^{\mu}(t)\rangle . \qquad \ldots (2.9)$$

Use of the thermal averages (2.6') and (2.9) in (2.4) yields

$$I_{iso}(\omega) = \frac{\omega^{(1)}(\omega^{(2)})^3}{2\pi c^4}\int_{-\infty}^{\infty} dt\, \exp(-i\omega t)\Big\{\langle (\overline{\alpha}^{\circ})^2\rangle + \sum_{\mu}\langle (\overline{\alpha}^{\mu})^2\rangle\langle q^{\mu}(0)\, q^{\mu}(t)\rangle\Big\} \qquad \ldots (2.4'a)$$

and $$I_{anis}(\omega) = \frac{\omega^{(1)}(\omega^{(2)})^3}{2\pi c^4}\int_{-\infty}^{\infty} dt\, \exp(-i\omega t)\Big\{\langle \tfrac{1}{10}\mathrm{Tr}[\overleftrightarrow{\beta}^{\circ}(0)\cdot\overleftrightarrow{\beta}^{\circ}(t)]\rangle$$

$$+ \sum_{\mu}\langle \tfrac{1}{10}\mathrm{Tr}[\overleftrightarrow{\beta}^{\mu}(0)\cdot\overleftrightarrow{\beta}^{\mu}(t)]\rangle\langle q^{\mu}(0)\, q^{\mu}(t)\rangle\Big\} \ldots (2.4'b)$$

The terms involving equilibrium polarisabilities ($\bar{\alpha}^{\circ}, \overleftrightarrow{\beta}^{\circ}$) correspond to Rayleigh scattering. In the present approximations, the isotropic Rayleigh scattering is elastic, since the Fourier transform of the time - constant $\langle(\bar{\alpha}^{\circ})^2\rangle$ is proportional to $\delta(\omega)$. The anisotropic Rayleigh scattering, however, is reorientationally broadened, because of the time dependence of $\overleftrightarrow{\beta}^{\circ}$ which arises through reorientation. The scattering terms involving polarisability derivatives ($\bar{\alpha}^{\nu}, \overleftrightarrow{\beta}^{\nu}$) correspond to vibrational Raman lines, the anisotropic components of which are broadened in a similar manner by reorientation. It might thus seem a matter of indifference, whether one attempts to study reorientation through Raman or through Rayleigh lineshapes. It will be recalled, however, that the above results presume the absence of angular correlations among neighbouring molecules, which, we have conceded, is a slender reed to lean on. Had we allowed for such correlations, cross terms between the polarisabilities of different molecules would have survived the process of ensemble averaging; the correlation functions which appear in (2.4') would represent only the "self" terms of a sum over all pairs of molecules. The appropriate generalization of (2.4') would include also the "distinct" terms, for each of which, the product occurring in every angular bracket of (2.4') is taken between quantities evaluated on two distinct molecules. At this point, a crucial difference can be discerned between the Raman and Rayleigh terms. It may still be argued that the distinct Raman terms vanish. Each such term contains a factor $\langle q_i^{\nu}(0)\ q_j^{\nu}(t)\rangle$, where i and j are distinct particle subscripts; this factor vanishes if, as might be expected, the vibrational phases of different molecules

are independent. Any correlation which persists despite the randomising effect of vibrational phases, is bound to be less important than that which infests the Rayleigh terms, on which no redeeming grace descends. Thus, the Raman spectrum will be a more faithful manifestation of the motion of an individual molecule than will the Rayleigh.

Granted that (2.4') holds, at least in regard to the Raman terms on each side of the equations, we focus attention on a single Raman vibrational line corresponding to the μ'th normal mode. So long as this line does not overlap significantly with any other line, we may, without serious inaccuracy, write

$$I^{\mu}_{iso}(\omega) = \frac{\omega^{(1)}(\omega^{(2)})^3}{2\pi c^4}\langle(\bar{\alpha}^{\mu})^2\rangle\int_{-\infty}^{\infty}dt\ \exp(-i\omega t)\langle q^{\mu}(0)q^{\mu}(t)\rangle$$

and $$I^{\mu}_{anis}(\omega) = \frac{\omega^{(1)}(\omega^{(2)})^3}{2\pi c^4}\cdot\frac{1}{10}\int_{-\infty}^{\infty}dt\ \exp(-i\omega t)\langle \mathrm{Tr}[\overleftrightarrow{\beta}^{\mu}(0)\cdot\overleftrightarrow{\beta}^{\mu}(t)]\rangle\langle q^{\mu}(0)q^{\mu}(t)\rangle\ ,$$

where I^{μ} denotes the truncated spectrum obtained by taking the actual scattering spectrum in some interval around the modal vibration frequency in question - large enough to include any measurable structure of this line, but small enough to exclude that of any other line - and by letting the spectrum vanish outside this interval. If we ignore the slow variation of $\omega^{(2)}$ within the interval, and regard the factors in front of the integrals as constants, then the spectra are evidently, within a multiplicative constant, Fourier transforms of the correlation functions occurring in the integrands, and conversely, the latter are, within a constant, inverse transforms of the spectra:

$$\hat{I}^{\mu}_{iso}(t) \sim \langle q^{\mu}(0)\, q^{\mu}(t)\rangle \qquad \ldots (2.10a)$$

and

$$\hat{I}^{\mu}_{anis}(t) \sim \langle \mathrm{Tr}[\overleftrightarrow{\beta}^{\mu}(0)\cdot\overleftrightarrow{\beta}^{\mu}(t)]\rangle\langle q^{\mu}(0)q^{\mu}(t)\rangle, \qquad \ldots (2.10b)$$

where

$$\hat{I}(t) \equiv \int_{-\infty}^{\infty} d\omega \exp(i\omega t)\, I(\omega).$$

Defining the "reorientational spectrum" $I_{or}(\omega)$ by the relation

$$\hat{I}^{\mu}_{or}(t) \sim \langle \mathrm{Tr}[\overleftrightarrow{\beta}^{\mu}(0)\cdot\overleftrightarrow{\beta}^{\mu}(t)]\rangle \qquad \ldots (2.11)$$

(the nomenclature is motivated by the orientation dependence of $\overleftrightarrow{\beta}$), we have from (2.10),

$$\hat{I}^{\mu}_{or}(t) \sim \hat{I}^{\mu}_{anis}(t)/\hat{I}^{\mu}_{iso}(t)\ . \qquad \ldots (2.12a)$$

The corresponding relation in the frequency domain, by the Fourier deconvolution theorem, is

$$I^{\mu}_{anis}(\omega) \sim I^{\mu}_{iso}(\omega) * I^{\mu}_{or}(\omega)\ , \qquad \ldots (2.12b)$$

where * denotes the folding operation.

Either of equations (2.12), together with (2.5), provides a way to extract I^{μ}_{or} , and the attendant information about molecular reorientation, from the data ($I_{\parallel}$ and $I_{\perp}$) which are available experimentally.

Having accomplished the separation of rotational from vibrational line broadening, we consider the effect of any other broadening influences, such as intermolecular collisions, which may be operative. An approach occasionally adopted[8,9] is to assume that non-reorientational broadening processes are statistically independent of the vibration

and reorientation, and that they contribute equally to the isotropic and anisotropic scattering. The effect of such processes is represented by modifying the polarisability derivatives ($\vec{\alpha}^{\mu}, \overleftrightarrow{\beta}^{\mu}$) by a multiplicative factor f(t). With f(t) taken to be uncorrelated with $q^{\mu}(t)$ and with orientation, (2.10) would be replaced by

$$\hat{I}^{\mu}_{iso}(t) \sim \langle q^{\mu}(0) q^{\mu}(t) \rangle \langle f(0) f(t) \rangle$$

and $$\hat{I}^{\mu}_{anis}(t) \sim \langle Tr[\overleftrightarrow{\beta}^{\mu}(0) \cdot \overleftrightarrow{\beta}^{\mu}(t)] \rangle \langle q^{\mu}(0) q^{\mu}(t) \rangle \langle f(0) f(t) \rangle ,$$

and (2.12) would follow as before. This method is not rigorous; one must therefore hope that non-reorientational broadening mechanisms are of secondary importance. The approach has, however, at least an instructive value, in that it emphasises the unique status of reorientation as the only broadening process under which $\vec{\alpha}^{\mu}$ may be expected to remain invariant. It is this feature which, in principle, enables a relatively simple separation of the reorientational spectrum.

IV. Rotational Diffusion -

Derivation of Diffusion Constants from Lineshapes:

Through equations (2.12) and (2.5), we have demonstrated the possibility of determining the reorientational spectrum from experiment. Our next objective is to use the information in the spectrum, quantitatively to characterise the reorientational motion itself. This will be accomplished through the derivation of rotational diffusion constants in terms of the linewidths of reorientational spectra.

From equation (2.11), and by our assumption that $\overleftrightarrow{\beta}^{\mu}$ depends only on molecular orientation, it is evident that $I_{or}(\omega)$ is determined in principle, once we have statistical knowledge of the time development of the angular distribution for an ensemble of molecules. The problem

of describing this time development is amenable to analysis if one considers that each molecule undergoes a large number of random rotations in any macroscopic time interval. Descriptions of molecular reorientation that conform to this pattern of motion are referred to as rotational Brownian motion models, in correspondence with the familiar case of microscopic translational motion in fluids, which likewise proceeds in random steps. Reorientation models in this category, which further stipulate that the individual angular steps are of small size, are more specifically designated as rotational diffusion models. This is because an ensemble of molecules, all prepared in the same initial orientation, and undergoing small-step rotational Brownian motion, will tend in the course of time to spread out in Euler angle space, in much the same way as particles undergoing translational Brownian motion tend to diffuse in ordinary space. In the case of translational Brownian motion, the size of individual step is immaterial to the nature of the motion - a change in the size of step affects only the length scale on which the phenomenon is viewed, without changing the equations that govern the motion. In the rotational case, however, a large step size results in a qualitatively different description of the motion, as compared with a small step size. That this difference might be expected, is suggested by the fact that angles are dimensionless quantities, so that a "large" angle cannot be made equivalent to a "small" angle by a change of scale.

Treatments of rotational Brownian motion which allow for large step sizes, have been offered[10,11] in the literature. These theories reproduce the results of rotational diffusion models in the small-step limit, and give at least formal solutions of the time development of the angular distribution, for arbitrary step size. They do not,

however, provide a simple interpretation of the motion on the basis of lineshape parameters, when they are applied to cases intermediate between the diffusion limit and the "free" (unhindered) rotation limit. The theory of Reference 11., moreover, is readily applicable only to linear and spherical top molecules. Accordingly, the following discussion will be confined to small-step diffusion.

A definitive treatment of rotational diffusion is given by Favro[12], who derives a quantum-statistical diffusion equation for anisotropic rotational motion, that is analogous to the classical Fokker-Planck equation for translational Brownian motion. Favro obtains,

$$\frac{\partial}{\partial t} P(\vec{\Omega},t) = -\sum_{jk} \hat{M}_j D_{jk} \hat{M}_k P(\vec{\Omega},t) . \qquad \ldots (2.13)$$

Here, $P(\vec{\Omega},t)\, d^3\Omega$ is the probability at time t, of finding a randomly chosen member of an ensemble of similar rigid bodies undergoing rotational diffusion, to be in the volume element $d^3\Omega$ of Euler angle space. Also, $\hat{M}_i$ is the i'th component of the "rotation" operator, which is related to the quantum-mechanical angular momentum operator $\hat{L}_i$ for a representative rotor, by

$$\hat{M}_i = \hbar^{-1} \hat{L}_i \quad . \qquad \ldots (2.14)$$

The D_{jk} form the components of the "diffusion tensor", defined by

$$D_{jk} \equiv \frac{1}{2\tau} \langle \epsilon_j \epsilon_k \rangle , \qquad \ldots (2.15)$$

where ϵ_i is the angular excursion about the i'th axis executed in the time τ, and where $\langle\,\rangle$ denotes an ensemble average. (It is assumed that $\langle \epsilon_j \epsilon_k \rangle$ is proportional to τ for sufficiently long τ, so that the D_{jk} are well defined. Also, it is assumed that a "sufficiently long" τ is

still short enough, that the ϵ_i remain essentially infinitesimal: the tensor transformation properties of the D_{jk} then follow from the vector character of small rotations $\vec{\epsilon}$.) The designation of the D_{jk} as "diffusion constants" is motivated by the relation, similar to (2.15), which holds for translational diffusion constants.[13]

To solve the angular distribution $P(\vec{\Omega},t)$, one seeks a Green's function or "evolution" function for (2.13), which will generate $P(\vec{\Omega},t)$ from a known initial distribution $P(\vec{\Omega},0)$. In terms of the Green's function G, one writes

$$P(\vec{\Omega},t) = \int d^3\Omega' \, P(\vec{\Omega}',0)\, G(\vec{\Omega}'|\vec{\Omega},t). \qquad \ldots(2.16)$$

Physically, one may expect a suitable G to exist, if the following superposition principle obtains: that the probability, that a rotor with given orientation $\vec{\Omega}'$ at time 0, will have reoriented into $d^3\Omega$ at time t, is independent of the initial angular distribution $P(\vec{\Omega}',0)$. For, then one may compute independently the contribution to $d^3\Omega$ at time t, from the population of each element $d^3\Omega'$ at time 0, as implied by (2.16).

Now, if (2.16) is to hold for arbitrary $P(\vec{\Omega}',0)$, then it is readily seen that, for any fixed $\vec{\Omega}''$, $G(\vec{\Omega}''|\vec{\Omega},t)$ must be a solution of the diffusion equation (2.13). This is shown by setting $P(\vec{\Omega}',0)$ equal to $\delta(\vec{\Omega}'-\vec{\Omega}'')$ in (2.16): then,

$$P(\vec{\Omega},t) = \int d^3\Omega' \, \delta(\vec{\Omega}'-\vec{\Omega}'')\, G(\vec{\Omega}'|\vec{\Omega},t) = G(\vec{\Omega}''|\vec{\Omega},t).$$

Since $P(\vec{\Omega},t)$ is a solution of (2.13) so is $G(\vec{\Omega}''|\vec{\Omega},t)$ for arbitrary $\vec{\Omega}''$.

Let us suppose that the operator

$$\hat{A} = \sum_{jk} \hat{M}_j \, D_{jk} \, \hat{M}_k$$

possesses a complete orthonormal set of eigenfunctions $\psi_n(\vec{\Omega})$, with corresponding eigenvalues λ_n. Then, for fixed $\vec{\Omega}'$ and t, $G(\vec{\Omega}'|\vec{\Omega},t)$ may be expanded in the $\psi_n(\vec{\Omega})$:

$$G(\vec{\Omega}'|\vec{\Omega},t) = \sum_n c_n(\vec{\Omega}',t)\, \psi_n(\vec{\Omega}) . \qquad \ldots (2.17)$$

Since $G(\vec{\Omega}'|\vec{\Omega},t)$ must satisfy (2.13), one may write

$$\sum_n \left[\frac{\partial}{\partial t} c_n(\vec{\Omega}',t)\right] \psi_n(\vec{\Omega}) = -\sum_n c_n(\vec{\Omega}',t)\, \hat{A}\, \psi_n(\vec{\Omega})$$

$$= -\sum_n \left[\lambda_n c_n(\vec{\Omega}',t)\right] \psi_n(\vec{\Omega}) .$$

By the orthogonality of the ψ_n, it is possible to equate their coefficients term-by-term:

$$\frac{\partial}{\partial t} c_n(\vec{\Omega}',t) = -\lambda_n c_n(\vec{\Omega}',t) .$$

Hence, $\quad c_n(\vec{\Omega}',t) = c_n^{\circ}(\vec{\Omega}')\, e^{-\lambda_n t}$.

Substitution into (2.17) yields

$$G(\vec{\Omega}'|\vec{\Omega},t) = \sum_n c_n^{\circ}(\vec{\Omega}')\, e^{-\lambda_n t}\, \psi_n(\vec{\Omega}) . \qquad \ldots (2.17')$$

The $c_n^{\circ}(\vec{\Omega}')$ are to be determined from the initial condition, that $P(\vec{\Omega},t) \rightarrow P(\vec{\Omega},0)$ as $t \rightarrow 0$, for arbitrary $P(\vec{\Omega},0)$. By (2.16), this condition will require

$$G(\vec{\Omega}'|\vec{\Omega},t) \rightarrow \delta(\vec{\Omega}'-\vec{\Omega}) \quad \text{as } t\rightarrow 0.$$

Also, by (2.17'),

$$G(\vec{\Omega}'|\vec{\Omega},t) \rightarrow \sum_n c_n^\circ(\vec{\Omega}')\,\psi_n(\vec{\Omega}) \quad \text{as } t\rightarrow 0.$$

Comparison of the last two results gives

$$\sum_n c_n^\circ(\vec{\Omega}')\,\psi_n(\vec{\Omega}) = \delta(\vec{\Omega}'-\vec{\Omega}).$$

If the ψ_n form a complete orthonormal set, we may invoke the completeness relation

$$\sum_n \psi_n^*(\vec{\Omega}')\,\psi_n(\vec{\Omega}) = \delta(\vec{\Omega}'-\vec{\Omega}),$$

so that $$\sum_n c_n^\circ(\vec{\Omega}')\,\psi_n(\vec{\Omega}) = \sum_n \psi_n^*(\vec{\Omega}')\,\psi_n(\vec{\Omega}).$$

Comparison of coefficients of the $\psi_n(\vec{\Omega})$ gives

$$c_n^\circ(\vec{\Omega}') = \psi_n^*(\vec{\Omega}'),$$

whereupon (2.17') becomes

$$G(\vec{\Omega}'|\vec{\Omega},t) = \sum_n \psi_n^*(\vec{\Omega}')\,e^{-\lambda_n t}\,\psi_n(\vec{\Omega}). \qquad \ldots (2.18)$$

Substitution into (2.16) yields the time development of the angular distribution:

$$P(\vec{\Omega},t) = \sum_n \left[\int d^3\Omega'\,P(\vec{\Omega}',0)\,\psi_n^*(\vec{\Omega}')\right]\psi_n(\vec{\Omega})\,e^{-\lambda_n t}. \qquad \ldots (2.16')$$

It remains to determine the eigenfunctions ψ_n of the operator

$\hat{A} = \sum_{jk} \hat{M}_j D_{jk} \hat{M}_k$. Referred to the principal axes of $\overleftrightarrow{D}$, the operator may be written, with the use of (2.14), as

$$\hat{A} = \sum_i (\hbar^{-2} D_i) \hat{L}_i^2 .$$

This is recognisable[14] as the quantum-mechanical Hamiltonian of a rigid rotor with principal moments of inertia $I_i = \hbar^2/2D_i$. Thus the ψ_n are merely the quantum-mechanical eigenfunctions of a rigid rotor with the same symmetry as that of the diffusion tensor. Since the symmetry of the molecular frame determines that of the diffusion tensor, the rotational diffusion of, say, a symmetric top molecule will be described by a Green's function constructed of symmetric top eigenfunctions.

It is well known[15] that the rigid rotor eigenfunctions are exactly soluble for spherical and symmetric tops (although only approximately for asymmetric tops). Moreover, for a symmetric top molecule, the eigenvalues λ_n of $\hat{A}$ are just the energy levels[15] E_n of the appropriate ($I_i = \hbar^2/2D_i$) symmetric top rigid rotor, and are thus related to the diffusion constants by

$$\lambda_n \rightarrow E_n = \frac{\hbar^2}{2I_1} J(J+1) + \frac{\hbar^2}{2}\left(\frac{1}{I_3} - \frac{1}{I_1}\right) K^2$$

$$\rightarrow J(J+1) D_1 + K^2 (D_3 - D_1) , \qquad \ldots (2.19)$$

where J and K are the rotational quantum numbers of ψ_n, and where the x_3 axis is the symmetry axis.

With knowledge of the ψ_n and of the λ_n, it is possible through (2.16') to calculate the correlation function $\langle Tr[\overleftrightarrow{\beta}^{\mu}(0) \cdot \overleftrightarrow{\beta}^{\mu}(t)] \rangle$ in (2.11).

To do so, one begins with an ensemble of molecules, all prepared, at time 0, with the same initial orientation $\vec{\Omega}''$. This corresponds to an angular distribution $P(\vec{\Omega}',0) = \delta(\vec{\Omega}'-\vec{\Omega}'')$, so that the subsequent distribution $P(\vec{\Omega},t)$, by (2.16') and (2.18), reduces to $G(\vec{\Omega}''|\vec{\Omega},t)$. Then, explicitly introducing the angular dependence of $\overleftrightarrow{\beta}^{\nu}$, one gets

$$\langle \mathrm{Tr}[\overleftrightarrow{\beta}^{\nu}(0)\cdot\overleftrightarrow{\beta}^{\nu}(t)]\rangle = \mathrm{Tr}[\overleftrightarrow{\beta}^{\nu}(\vec{\Omega}'')\cdot\langle\overleftrightarrow{\beta}^{\nu}(\vec{\Omega}(t))\rangle]$$

$$= \mathrm{Tr}[\overleftrightarrow{\beta}^{\nu}(\vec{\Omega}'')\cdot\int d^3\Omega\, G(\vec{\Omega}''|\vec{\Omega},t)\,\overleftrightarrow{\beta}^{\nu}(\vec{\Omega})].$$

Valiev[16] evaluates this expression, using (2.18) for $G(\vec{\Omega}''|\vec{\Omega},t)$, and using the transformation properties of tensors in the spherical basis to find $\overleftrightarrow{\beta}^{\nu}(\vec{\Omega})$ from $\overleftrightarrow{\beta}^{\nu}(\vec{\Omega}'')$. Valiev's result for a symmetric top expresses the correlation function as a linear combination of exponentials:

$$\langle \mathrm{Tr}[\overleftrightarrow{\beta}^{\nu}(0)\cdot\overleftrightarrow{\beta}^{\nu}(t)]\rangle = k_1 \exp[-6D_\perp|t|] + k_2\exp[-(5D_\perp+D_\parallel)|t|]$$

$$+k_3\exp[-(2D_\perp+4D_\parallel)|t|], \qquad \ldots (2.20)$$

where the k_i are functions of the components of $\overleftrightarrow{\beta}^{\nu}(\vec{\Omega}'')$, and where $D_1 = D_2 = D_\perp$, and $D_3 = D_\parallel$. (The diffusion constants enter the expression through (2.19).)

Some simplification of (2.20) may occur if a specific normal vibration mode is considered. In the particular instance of an A_{1g} (totally symmetric) vibration in a D_{6h} (symmetric top) molecule, it is found[7] that k_2 and k_3 vanish, so that for the case of interest in the present work, viz., the 992 cm.$^{-1}$ A_{1g} line of benzene, we have

$$\langle \mathrm{Tr}[\overleftrightarrow{\beta}^{\nu}(0)\cdot\overleftrightarrow{\beta}^{\nu}(t)]\rangle \sim \exp[-6D_\perp|t|], \qquad \ldots (2.20')$$

whence the correlation function is exponential with a decay time or "correlation time"

$$\tau_c = (6 D_\perp)^{-1} . \qquad \ldots (2.21)$$

This reduction is, indeed, expected. A totally symmetric vibration preserves the symmetry of the molecular frame, so that $\overleftrightarrow{\beta}^{\nu}$ must have the same (symmetric top) symmetry as has the molecular frame. Thus, $\overleftrightarrow{\beta}^{\nu}$ should be invariant under reorientations about the molecular symmetry axis. It is these reorientations that are characterised by $D_{\parallel}$; therefore, $D_{\parallel}$ should be absent from the expression for $\langle Tr[\overleftrightarrow{\beta}^{\nu}(0)\cdot\overleftrightarrow{\beta}^{\nu}(t)]\rangle$. For the benzene line in question, the reorientational spectrum is a manifestation solely of the "tumbling" motions about axes perpendicular to the symmetry axis.

It is now apparent that the study of Raman vibrational lines of different symmetry species, insomuch as it furnishes the correlation functions $\langle Tr[\overleftrightarrow{\beta}^{\nu}(0)\cdot\overleftrightarrow{\beta}^{\nu}(t)]\rangle$, may lead to the determination of the complete diffusion tensor - provided, of course, that the reorientational motion is well represented by rotational diffusion.

A final point of considerable importance, is that the correlation time of (2.21) is readily obtainable from the frequency profile of the reorientational spectrum, without recourse to the time domain. The spectrum, by (2.11), is the Fourier transform of (2.20'). The Fourier transform of an exponential with time constant τ_c, is a Lorentzian with a full width at half-maximum (FWHM) of $\Gamma = 2/\tau_c$ in units of angular frequency, or

$$\Gamma = (\pi c \tau_c)^{-1} , \qquad \ldots (2.22)$$

where c is the speed of light, if Γ is measured in wavenumbers ($cm.^{-1}$).

Using (2.21), we may express the linewidth (FWHM) of the reorientational spectrum, for a totally symmetric vibration of a symmetric top molecule:

$$\Gamma_{or} = 6(\pi c)^{-1} D_{\perp} , \qquad \ldots (2.23a)$$

or conversely

$$D_{\perp} = \frac{1}{6}\pi c \Gamma_{or} . \qquad \ldots (2.23b)$$

With this result, we have accomplished the objective, of deriving diffusion constants from lineshape parameters.

V. <u>Significance of Rotational Diffusion Constants - Relation of Diffusion Constants to Friction Constants:</u>

Our purpose in this section is to interpret the rotational diffusion constants of IV., in terms of the torques which couple a rotating molecule to its environment and which therefore (given that the fluid does not rotate bodily) tend systematically to hinder the reorientations of the molecule. Although the connection between rotational diffusion and rotational friction constants will be derived below in a concrete and specific fashion, it may be appreciated in the abstract as a consequence of the fluctuation-dissipation theorem.

We begin by recasting the definition of the diagonal diffusion constants in a form involving a correlation function of angular velocity. This is done in a manner similar to a treatment by Zwanzig[17] of translational diffusion. In consequence of (2.14), the diagonal elements of the diffusion tensor $\overleftrightarrow{D}$ may be written

$$D_i = \frac{1}{2\tau}\langle \epsilon_i(\tau)\epsilon_i(\tau)\rangle ,$$

when D_i and ϵ_i are referred to the principal axes of the diffusion tensor. One may replace $\epsilon_i(\tau)$ by

$$\epsilon_i(\tau) = \int_0^\tau dt\ \omega_i(t) \ ,$$

where ω_i is the angular velocity about the i'th principal axis of the diffusion tensor:

$$D_i = \frac{1}{2\tau}\left\langle \left[\int_0^\tau dt'\ \omega_i(t')\right]\left[\int_0^\tau dt''\ \omega_i(t'')\right]\right\rangle$$

$$= \frac{1}{2\tau}\int_0^\tau dt' \int_0^\tau dt'' \left\langle \omega_i(t')\,\omega_i(t'')\right\rangle .$$

The integration domain may be separated into the two regions $t' < t''$ and $t'' < t'$, the integrals over which are equal by the symmetry in t' and t".

$$\therefore\ D_i = \frac{1}{\tau}\int_0^\tau dt' \int_{t'}^\tau dt'' \left\langle \omega_i(t')\,\omega_i(t'')\right\rangle .$$

With the transformation t = t" - t', this becomes

$$D_i = \frac{1}{\tau}\int_0^\tau dt' \int_0^{\tau - t'} dt \left\langle \omega_i(t')\,\omega_i(t'+\tau)\right\rangle .$$

The ensemble average may be assumed "stationary" - i.e., invariant under shifts of the time origin, and therefore dependent only on t, not on t'. Also, τ is essentially infinite on the time scale of characteristic molecular processes, since it must be great enough to accommodate a statistically large number of random steps for the diffusion constant to be well defined. This permits the upper limit of the inner integral to be replaced by ∞. Thus, the inner integral is independent of t':

$$D_i = \frac{1}{\tau}\int_0^{\tau} dt' \int_0^{\infty} dt \langle \omega_i(0)\, \omega_i(t)\rangle$$

$$= \int_0^{\infty} dt \langle \omega_i(0)\, \omega_i(t)\rangle . \qquad \ldots (2.24)$$

Next, we evaluate the angular velocity correlation function through an investigation of the rotational dynamics of the molecule.

Following Steele[18], we treat the molecule as a classical rigid rotor, described by Euler's equations[19]:

$$I_x \dot{\omega}_x - \omega_y \omega_z (I_y - I_z) = N_x \;;$$

$$I_y \dot{\omega}_y - \omega_x \omega_z (I_z - I_x) = N_y \;;$$

$$I_z \dot{\omega}_z - \omega_y \omega_x (I_x - I_y) = N_z \;.$$

Here, I_i is the i'th principal moment of inertia; $\vec{\omega}$ is the angular velocity, referred to the principal axes of the molecule (that is, evaluated in a non-rotating frame whose axes instantaneously coincide with those of the molecule); $\vec{N}$ is the instantaneous torque, again referred to the molecular axes.

By analogy with the well known treatment of translational diffusion via the Langevin equation[20], we assign to $\vec{N}$ the phenomenological form

$$\vec{N} = -\overleftrightarrow{\xi} \cdot \vec{\omega} + \vec{N}'(t) ,$$

where $\overleftrightarrow{\xi}$ is the rotational drag tensor, which is constant when referred to the molecular axes and is responsible for the systematic tendency of the rotor toward equilibrium, and where $\vec{N}'(t)$ is a rapidly fluctuating torque arising from random changes in the molecular environment of the

rotor. Now, $\overleftrightarrow{\xi}$ must exhibit all the symmetries of the molecule, since it is characteristic of the molecule itself and independent of environmental fluctuations. It follows that the principal axes of $\overleftrightarrow{\xi}$ coincide with those of the inertia tensor; thus $\overleftrightarrow{\xi}$ is diagonal in the same frame as is $\overleftrightarrow{I}$. In terms of the diagonal elements ("friction constants") of $\overleftrightarrow{\xi}$, the Euler equations become

$$I_x\dot{\omega}_x - \omega_y\omega_z(I_y - I_z) = -\xi_x\omega_x + N_x'(t) \qquad \text{et cyc.}$$

Even with this simplification, the equations are not generally soluble in closed form for arbitrary values of the I_i . Nonetheless, they become trivial for the case of a spherical top rotor, which is treated by Steele[18] and Hubbard[21]. In this case, the Euler equations are uncoupled, since the cross terms in the angular velocities vanish.

It has been suggested[22], that if only systems whose reorientation is of a strongly diffusive nature are considered, then it is permissible to neglect the crossterms, even for an asymmetric top. When the motion follows a pattern of small-step rotational diffusion, it is clear that the frequent sharp changes of rotational direction, executed by the molecule in the course of small angular displacements, are indicative of angular accelerations that are large in relation to angular velocities. Thus, the neglect of cross terms in the ω_i , in favour of terms in the $\dot{\omega}_i$, is plausible in the diffusion limit.

Upon deletion of the cross terms, the stochastic equations governing reorientation reduce to the uncoupled form

$$\dot{\omega}_i = [-\xi_i\omega_i + N_i'(t)]/I_i \quad , \quad i = x, y, z ,$$

which is formally identical to the Langevin equation. This is a linear,

first order, inhomogeneous differential equation, with solution

$$\omega_i(t) = \exp(-\xi_i t/I_i) \times \left[\omega_i(0) + \frac{1}{I_i}\int_0^t dt' N_i'(t') \exp(\xi_i t'/I_i)\right].$$

Knowledge of the time dependence of ω_i enables us to evaluate the correlation function $\langle \omega_i(0)\, \omega_i(t)\rangle$:

$$\langle \omega_i(0)\, \omega_i(t)\rangle = \langle \omega_i^2(0)\rangle \exp(-\xi_i t/I_i)$$

$$+ \frac{1}{I_i} \exp(-\xi_i t/I_i) \int_0^t dt' \exp(\xi_i t'/I_i) \langle N_i'(t')\rangle .$$

Since $\vec{N}'(t)$ is purely random, we may assume $\langle \vec{N}'(t')\rangle = 0$, whence

$$\langle \omega_i(0)\, \omega_i(t)\rangle = \langle \omega_i^2(0)\rangle \exp(-\xi_i t/I_i) . \qquad \ldots (2.25)$$

It is simple to evaluate $\langle \omega_i^2(0)\rangle$ from statistical mechanics. The kinetic energy of a rotor, evaluated in the principal axis frame, is[19] $\frac{1}{2}(I_1\omega_1^2 + I_2\omega_2^2 + I_3\omega_3^2)$. Thus, the energy associated with rotation about the i'th axis is $\frac{1}{2} I_i \omega_i^2$. By the equipartition theorem,

$$\langle \tfrac{1}{2} I_i \omega_i^2(0)\rangle = kT/2 \qquad , \text{ or } \quad \langle \omega_i^2(0)\rangle = kT/I_i .$$

Equation (2.25) becomes

$$\langle \omega_i(0)\omega_i(t)\rangle = \frac{kT}{I_i} \exp(-\xi_i t/I_i) . \qquad \ldots (2.25')$$

Since the diffusion tensor, like the drag tensor, shares the symmetries of the molecule, its principal axes coincide with those of the inertia tensor; (2.24) and 2.25') therefore hold in the same frame of reference. Substitution of (2.25') into (2.24) yields

$$D_i = \frac{kT}{I_i}\int_0^\infty dt \exp(-\xi_i t/I_i)$$

$$= kT/\xi_i \quad . \qquad \ldots (2.26)$$

This establishes the relation between diffusion and friction constants. The present result parallels that deduced by Einstein (1905) for the translational diffusion of a Brownian particle.

References:

1. R. G. Gordon, J. Chem. Phys. 42, 3658 (1965).
2. G. Placzek, "The Rayleigh and Raman Scattering", UCRL Trans. 526(L), (Clearinghouse for Federal and Scientific Information, Department of Commerce, 1959).
3. G. Baym, "Lectures on Quantum Mechanics" (W. A. Benjamin, Inc., Reading, Mass., 1969), p. 134.
4. Ibid., p. 136.
5. W. A. Steele in "Transport Phenomena in Fluids", edited by H. J. M. Hanley (Marcel Dekker, New York and London, 1969), p. 275.
6. L. A. Nafie and W. L. Peticolas, J. Chem. Phys. 57, 3145 (1972).
7. F. J. Bartoli and T. A. Litovitz, J. Chem. Phys. 56, 413 (1972).
8. R. B. Wright, M. Schwartz, and C. H. Wang, J. Chem. Phys. 58, 5125 (1973).
9. J. H. Campbell, J. F. Fisher, and J. Jonas, J. Chem. Phys. 61, 346 (1974).
10. E. N. Ivanov, Sov. Phys. JETP 18, 1041 (1964).
11. R. G. Gordon, J. Chem. Phys. 44, 1830 (1966).
12. L. D. Favro, Phys. Rev. 119, 53 (1960).
13. F. Reif, "Fundamentals of Statistical and Thermal Physics" (McGraw-Hill, Inc., New York, 1965), p. 488.
14. I. N. Levine, "Quantum Chemistry", Vol. II (Allyn and Bacon, Boston, 1970), p. 208.
15. Ibid., pp. 211-220.
16. K. A. Valiev, Opt. Spectry. (USSR) 13, 282 (1962).
17. R. Zwanzig, Ann. Rev. Phys. Chem. 16, 67 (1965).
18. W. A. Steele, J. Chem. Phys. 38, 2404 (1963).
19. L. D. Landau and E. M. Lifshitz, "Mechanics" (Permagon Press, Oxford, 1960).
20. Reference 13., pp. 560-567.
21. P. S. Hubbard, Phys. Rev. 131, 1155 (1963).
22. W. T. Huntress, Jr., Advan. Magnetic Resonance 4, 1 (1970).

CHAPTER 3

EXPERIMENTAL ASPECTS

In its essentials, the experimental setup was typical of Raman scattering systems. Most individuating features arose from the necessity, in the present work, to minimize the entry of stray light from the strong isotropic scattering, into the measurement of the weak anisotropic scattering.

The system was constituted as follows (Fig. 1): The linearly polarised beam from a laser light source was brought to a weak focus within a sample cell. The cell was located in a temperature-regulated enclosure. Spherical collection optics, with an axis at right angles to the beam, viewed the light scattered at the beam focus, analyzed it according to polarisation, and imaged the light of the selected polarisation onto the entrance slit of a spectrometer. The light passed by the spectrometer was detected by a photomultiplier tube, the signal from which was processed by digital (photon-counting) electronics.

It will be convenient to discuss experimental aspects in relation to the various system elements mentioned in the above paragraph (Part A.). This discussion will be supplemented by some notes on methods (Part B.).

A. The Experimental Setup

1. Light source and pre-sample optics:

The light source was a CRL #52 argon ion Laser, operating at about 1/4 watt on the 4880 Å. line. It was equipped with a Brewster angle window, which so polarised the beam that its electric vector was perpendicular to the direction of observation. Isotropically scattered light would thus propagate with maximum intensity along

FIG. 1

Block diagram of the apparatus.

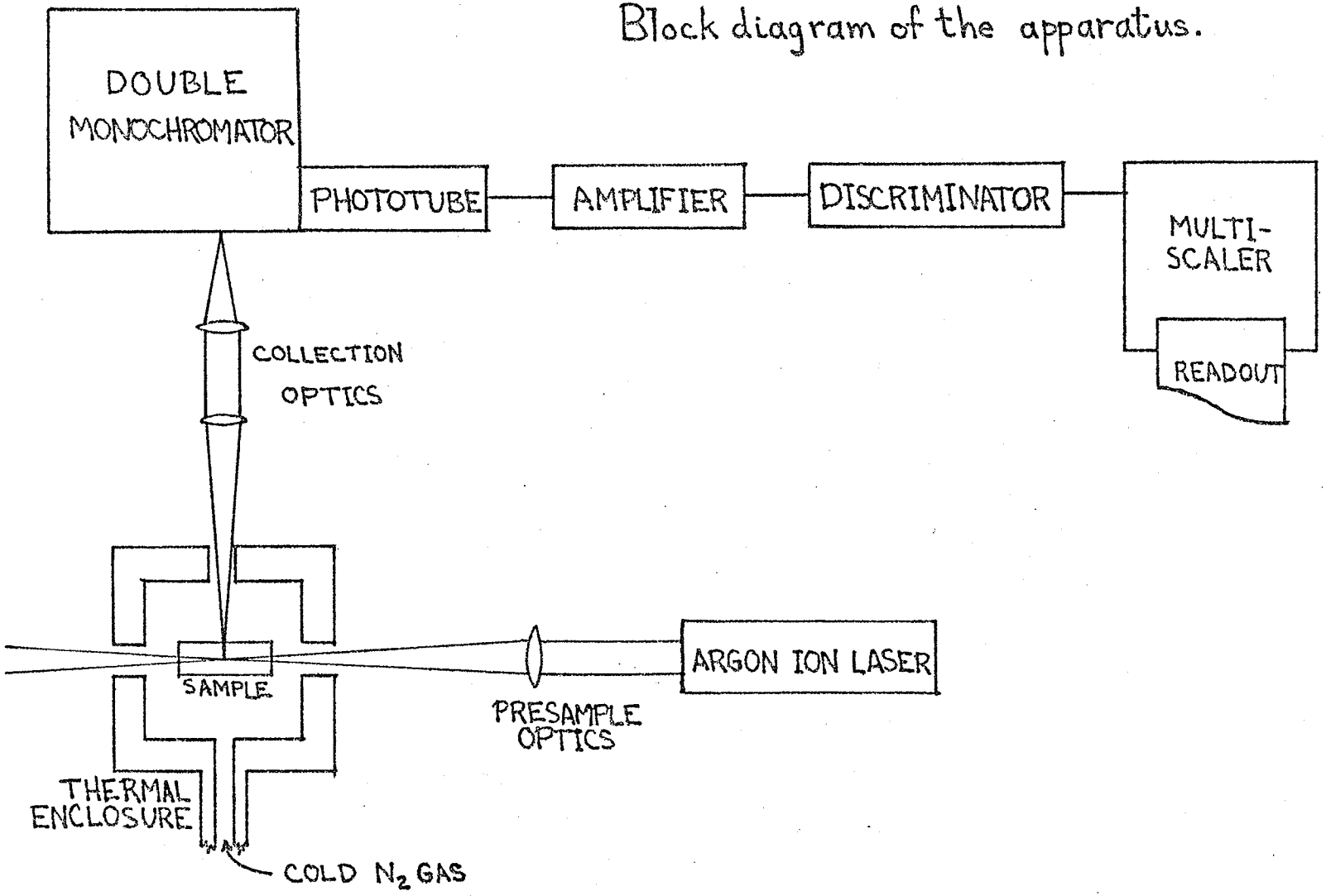

the observation direction, with its mode of polarisation unchanged in the scattering process. This arrangement afforded the freedom to pass, or to extinguish, the isotropic component, by means of setting the analyser to transmit light polarised, respectively, parallel or perpendicular to the electric vector of the beam.

A lens of focal length 30 cm., placed in the incident beam, brought the beam to a weak focus within the sample. Although a shorter focal length, according to a study by Schwiesow[1], would be desirable from the standpoint of maximum light collection, the longer focus was selected to preserve a well-defined beam polarisation. Otherwise no setting of the analyser would entirely block the transmission of isotropically scattered light.

2. Sample cell and collection optics:

The focused, linearly polarised beam was incident on a rectangular, fused quartz cell containing the liquid sample. Since fused quartz has no definite crystal structure, passage through the cell walls would not depolarise the beam, nor the scattered light.

The axis of the collection optics was at right angles to the beam. This scattering geometry reduces stray scattered light, and facilitates depolarisation measurements.[2]

A diaphragm, placed in front of the collection optics, limited light collection to a cone subtending 4° planar angle at the beam focus. The value 4° has been suggested[3] as an upper limit, since for larger collection angles, the isotropic scattering would lose some polarisation definition, and could not be extinguished entirely at any setting of the analyser.

The light cone was rendered parallel by a collimator lens, then presented to an analyser of sheet polaroid in a rotatable mount, whose extinction ratio was measured to be better than 10^{-4}. (Analyser light leak would not, at this value, contribute a significant amount of stray light.) A second lens focused the light onto the entrance slit of the spectrometer. The two lenses were chosen and arranged so that the light they passed would not overfill the acceptance cone of the spectrometer; otherwise, signal losses would occur.

3. The spectrometer:

The light was dispersed by a Jarrell-Ash 25-100 Series scanning spectrometer. This instrument consists of two grating monochromators in tandem, in the Czerny-Turner configuration. (The double monochromator design improves stray light rejection - "stray" light being, in this context, light of the wrong frequency, rather than of the wrong polarisation mode, as the term has heretofore been construed.) It was equipped with a grating drive linear in wavenumber, which divided an advance of 1 $cm.^{-1}$ into 20 mechanical steps.

4. Signal detection and processing:

Light passed by the spectrometer was detected by an RCA C31034 photomultiplier tube, cooled to -20° C. This tube was selected for its low dark noise, high quantum efficiency, and broad range of flat spectral sensitivity. It was followed by pulse-counting electronics, which enjoy several advantages[2] over conventional phase-sensitive amplification systems:

(a) Elimination of drift problems in electronics.

(b) Linear response to light intensity over a large dynamic range, due to the high-frequency response of electronic pulse circuitry.

(c) Direct digital output is possible, and convenient for digital data processing. In the present work, spectra were recorded digitally by a Victoreen ST400M multi-channel analyser (used in the multi-scaler mode).

(d) Discrimination against noise pulses originating in the phototube dynodes is possible. These pulses, due to secondary electrons emitted by the dynodes, have a smaller mean height than genuine signal pulses. Since individual pulses are handled separately, small pulses can be distinguished as such and blocked by a discriminator. In the present work, the discriminator level was set in accordance with the criterion set forth by Young[4] for optimal signal-to-noise ratio in the "low-signal limit".

5. Sample temperature control:

The sample cell reposed in a thermally insulated enclosure, into which cold N_2 gas was ducted. The continuous flow of cold, dry gas both regulated the sample temperature and prevented fogging of the sample cell. The gas was evolved by boiling off liquid N_2 electrically, at a rate governed by negative feedback from a thermistor in contact with the sample cell (Fig. 2). A temperature operating point was established when equilibrium was reached: feedback produced a gas flow just sufficient to maintain the current sample temperature. Any change in temperature was buffered (not wholly offset) by an opposing change in flow rate. This arrangement fell short of a true closed-loop control system[5], which would have a null output when the selected operating point were reached, and would act to restore the operating point once a critical deviation were exceeded. The cycling character of such a system, however, would introduce stability problems absent from the former arrangement.

FIG. 2

Circuit diagram of temperature regulator.

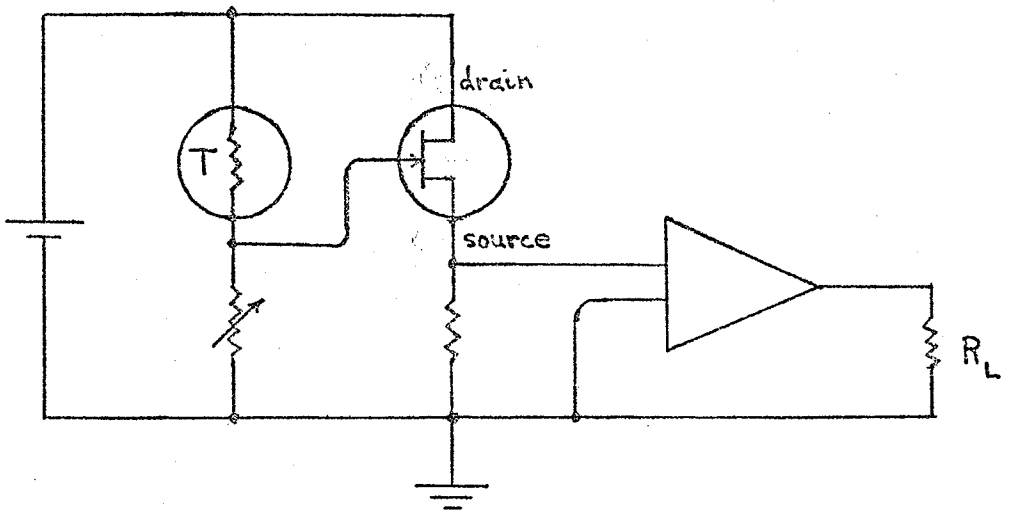

R_L is the load resistance.
Cold N_2 gas is evolved by the heat dissipated across R_L.

The regulating characteristics were appraised from the following point of view. First, one defines a "terminal sample temperature" T_∞ as that which would be reached if a given output level L were sustained indefinitely. The schedule $T_\infty(L)$ (Fig. 3a) depends parametrically on some set of ill-controlled variables $\{a_j\}$ - ambient temperature, etc. The purpose of the regulator is to suppress any excursions of the operating temperature T_{op}, which accompany drifts in $\{a_j\}$. To assess how effectively this is accomplished, one considers the output level L as a function $L(T_i)$ of the instantaneous sample temperature, the dependence arising through feedback. This schedule (Fig. 3b) is fixed once the design characteristics of the regulator, and any settings made to choose the operating temperature, are specified. A third function $T_\infty(T_i)$ is constructed by composing $T_\infty(L)$ with $L(T_i)$. Through $T_\infty(L)$, it depends parametrically on $\{a_j\}$. The significance of this schedule is that, if the current sample temperature is T_i, then the output level is such as to make the sample temperature tend toward $T_\infty(T_i)$. Equilibrium is realized, and an operating point established, when $T_\infty(T_i) = T_i$ (Fig. 3c). Approximately, $T_\infty(T_i)$ may be regarded as linear near the operating point. Also, the effect of a change in $\{a_j\}$ may be regarded approximately as a uniform shift of the schedule $T_\infty(T_i)$ through ΔT along the T_∞ axis (Fig. 3a). The corresponding change x in T_{op}, if m be the slope of $T_\infty(T_i)$, is given by

$$x - mx = \Delta T, \qquad \text{or} \qquad x = \Delta T/(1-m),$$

as is evident upon inspection of Fig. 3d. But ΔT is just the "open loop" temperature change that would be sustained if $\{a_j\}$ shifted and L remained constant (i.e., in the absence of feedback modulation). Hence $1/(1-m)$ represents the factor by which temperature drifts are suppressed

FIG. 3

Graphical analysis of temperature regulation.

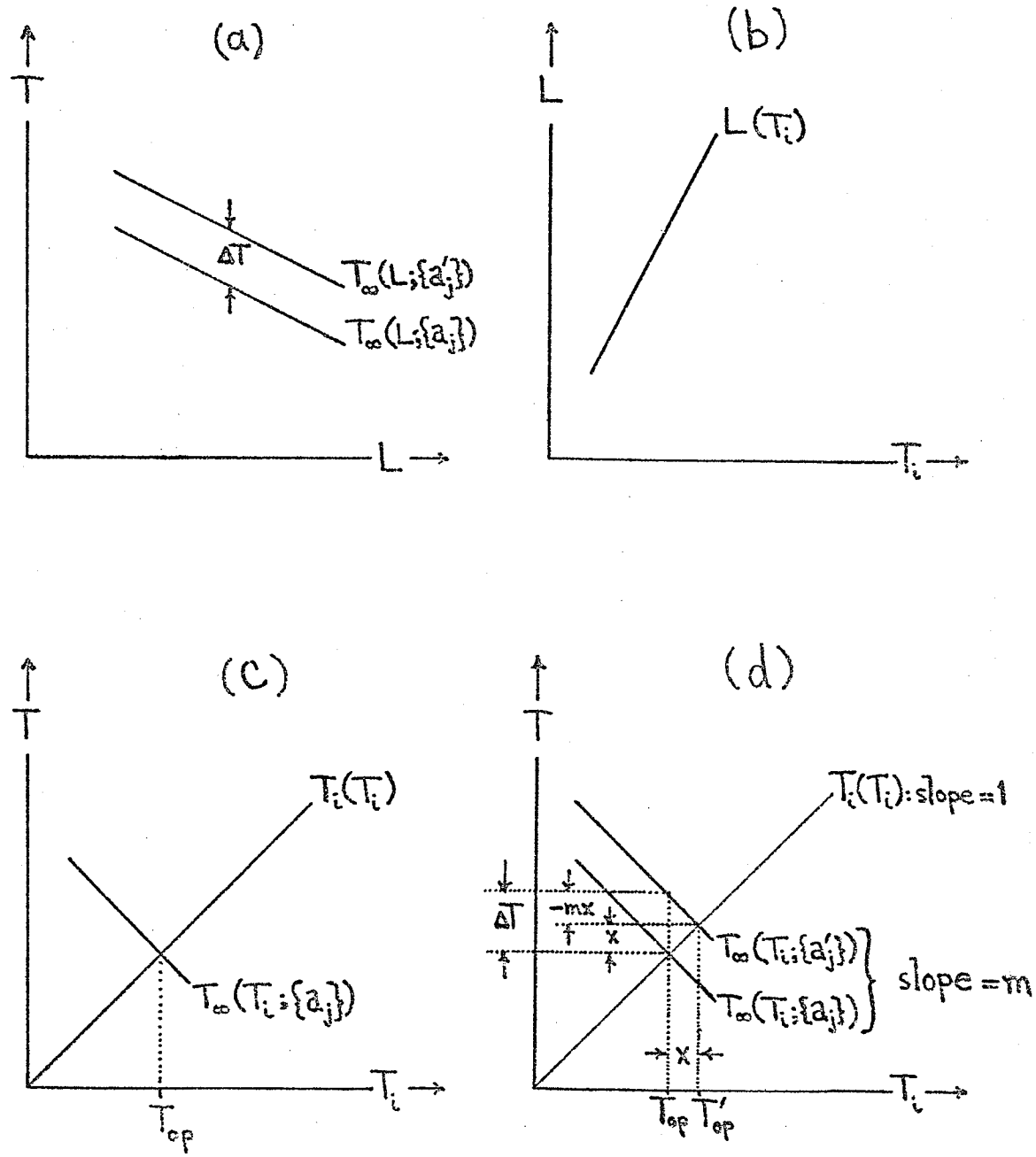

by feedback, and as such is an index of the performance of the regulator.

Now, m is computable:

$$m = dT_\infty / dT_i = (dT_\infty / dL) \cdot (dL/dT_i).$$

An empirical determination of dT_∞/dL was made by plotting equilibrium temperatures against the corresponding output levels (i.e., voltages across the heating element R of Fig. 2). Moreover, dL/dT_i, the voltage change per degree change of sample temperature, at fixed control settings, was calculable from the characteristic of the thermistor and from the gain of the amplifier circuit. On this basis, it was estimated that $m \simeq -10$, so that temperature drifts were suppressed by a factor $1/(1-m) \simeq .1$, in the operating region.

B. Methods

1. Measurement of the instrumental profile:

A high degree of spectral resolution can be attained only if the spectral slit width is made narrow in relation to the structures being examined. The loss of signal strength which attends a reduction in slit width, forces a compromise between resolution and signal level. In the present work, the weakness of the depolarised light signal, especially at lower C_6H_6 concentrations, necessitated the use of slit widths broad enough to produce measurable distortion of the spectra. Accordingly, some form of instrumental correction was called for. Any such correction requires the measurement of the "slit function" - the distribution in indicated frequency, of unit intensity of monochromatic light passed by the spectrometer.

Slit functions were obtained by allowing the spectrometer to observe the Tyndall scattering from an aluminum surface, of the (closely monochromatic) laser beam, while scanning over the laser line frequency.

New profiles were taken every day the experiment was in progress, and every time slit widths were changed.

2. Sample preparation:

The chemicals (C_6H_6 and CCl_4) used as samples, were supplied by the J. T. Baker Chemical Co., and were certified as being of GC spectrophotometric quality. Mixtures were prepared volumetrically, and allowed to stand an hour or so to ensure homogeneity. They were then introduced to the sample cell, through a syringe equipped with a membrane filter of pore diameter .2 μ. Filtration removed any dust particles which might cause Tyndall scattering while floating through the laser beam. The quoted mole fractions of C_6H_6 for the various mixtures, are estimated to be correct within, at worst, 3%.

3. Considerations related to frequency matching of polarised with depolarised spectra:

Spectra were taken in an alternating sequence of polarised and depolarised scans. In each such pair of runs, the same frequency interval was scanned - insofar as the apparatus behaved reproducibly on successive scans - and explicit experimental parameters (temperature, concentration) were held constant, so that the pair of spectra could be superposed along the frequency axis, and analyzed together. (In point of fact, some frequency mismatch appeared to persist, so that satisfactory results could not be obtained without the introduction of an analytical correction: this matter will be dealt with in Ch. 4.) Slit widths were also held constant in each pair of spectra, to permit the application of one of the modes of linewidth analysis to be described in Ch. 4. The large slit widths required for the depolarised spectra (as discussed under 1.), wrought grievous distortion of narrow polarised

structures, and in fact required the use of neutral density filters to reduce the polarised light signal to a level at which the electronics could accommodate it.

4. Measurement of stray light:

Notwithstanding such measures, alluded to in A., as were taken in aid of stray light reduction, a significant stray light contribution was manifest in the depolarised spectra, and an analytical correction was necessary. This would take the form,

$$I_{\perp}^{t}(\omega) = I_{\perp}^{m}(\omega) - c\, I_{\parallel}^{m}(\omega) ,$$

where the superscripts 't' and 'm' denote, respectively, 'true' and 'measured', and c is constant.

A procedure suggested by Bartoli and Litovitz[6] was followed, in an attempt to determine c as a "cell constant", or characteristic of the experimental setup. An apparent depolarisation ratio

$$\rho^{m} = \frac{\int I_{\perp}^{m}(\omega)\, d\omega}{\int I_{\parallel}^{m}(\omega)\, d\omega} = \frac{\int I_{\perp}^{t}(\omega)\, d\omega + c\int I_{\parallel}^{m}(\omega)\, d\omega}{\int I_{\parallel}^{m}(\omega)\, d\omega}$$

was measured for the 459 $cm.^{-1}$ Raman band of CCl_4 . This was compared to the value which should have been measured in the absence of stray light:

$$\frac{\int I_{\perp}^{t}(\omega)\, d\omega}{\int I_{\parallel}^{m}(\omega)\, d\omega} = \rho^{t} \times \frac{e_{\perp}}{e_{\parallel}} ,$$

where ρ^{t} is the actual depolarisation ratio, obtained from the literature[7], and $e_{\perp}$, $e_{\parallel}$ are grating efficiencies for the $\perp$ and $\parallel$ polarisations. Evidently,

$$c = \rho^{m} - \rho^{t} \times \frac{e_{\perp}}{e_{\parallel}} .$$

This determination of c would seem to be of doubtful reliability, in that the theoretical depolarisation ratio on which it depends is not known with great accuracy. Moreover, even the objective, by any means, of making a single master measurement of c, is open to question: for in the course of different experiments, variations in, say, index of refraction among various liquids at various temperatures, might lead to different c values.

In preference to reliance on this measurement, an analytical technique was adopted to associate a value of c with each individual experiment. This will be discussed in Ch. 4.

5. Selection of temperature range:

Some caution had to be exercised in selecting the range of sample temperatures over which the experiments were carried out. Benzene and CCl_4 form a eutectic mixture in which, for some relative concentrations, dimerisation may occur at sufficiently low temperatures.[8] It would be possible, if dimerisation were allowed to occur, that some of the depolarisation of the benzene vibrational line were due to reorientations, not of the benzene molecule, but of the dimer. For this reason, sample temperatures were kept high enough to avoid significant dimerisation.

References:

1. R. L. Schwiesow, J. Opt. Soc. Am. 59, 1285 (1969).
2. J. J. Barrett and N. I. Adams, III, J. Opt. Soc. Am. 58, 311 (1968).
3. J. E. Griffiths, J. Chem. Phys. 59, 751 (1973).
4. A. T. Young, Applied Optics 8, 2431 (1969).
5. S. M. Shinners, "Modern Control System Theory and Application" (Addison-Wesley, Reading, Mass., 1972).
6. F. J. Bartoli and T. A. Litovitz, J. Chem. Phys. 56, 404 (1972).
7. W. F. Murphy, M. V. Evans, and P. Bender, J. Chem. Phys. 47, 1836 (1966).
8. W. F. Wyatt, Trans. Faraday Soc. 25, 48 (1929).

CHAPTER 4

LINEWIDTH ANALYSIS

The determination of correlation times through linewidths, especially for the reorientational spectra, presented by no means a trivial problem. We consider that the analytical methods which were employed merit a full accounting. One reason is that two distinct approaches to the analysis of reorientational spectra were adopted, of which, one yielded satisfactory results, whereas the other tended systematically to overestimate the linewidth. We remain, at this writing, uncertain of the cause of failure of the latter method, which has been used with apparent success in the literature. Accordingly, we feel obliged to make a record of our procedures, in the hope that outside scrutiny may elucidate the nature of our difficulties. The other reason, less dolorous to report, is that we have brought to bear on the problem of linewidth analysis, several techniques which, if not original, have at least been developed independently in the course of this work - and which, we concede, may have contributed to the aforementioned difficulties.

Since the major impediments to our program of linewidth analysis arose in connection with the reorientational spectra, most of the following discussion will deal with these spectra. The vibrational relaxation spectra will be treated somewhat parenthetically. Suffice it to say, at the outset, that the arsenal to be directed at the reorientational spectra is adequate to deal with the vibrational spectra: the only major problem encountered in analysis of the latter, is the deconvolution of the instrumental profile from the spectra.

We begin by noting that, if it is expected that a spectrum will be determined by an exponential time correlation function, then two broad avenues may be followed toward the calculation of correlation times:
(1) Time domain: The Fourier transform of the spectrum may be taken; the resulting correlation function may then be fit to an exponential test function, whose decay time τ may be identified with the correlation time.
(2) Frequency domain: The spectrum may be fit directly to a Lorentzian, whose width stands in the relation $\Gamma \sim 1/\tau$ to the correlation time.

The statements that the spectrum $I(\omega)$ is Lorentzian, and that its Fourier transform $\hat{I}(t)$ is exponential, are mathematically equivalent. It follows, according to Wright et al.[1], that the approximations inherent in methods (1) and (2) are identical. The second approach was elected, since it entails only a fitting operation, while the other requires both that and a Fourier transformation.

Fitting of the spectra was accomplished by the well known non-linear least squares technique of linearisation of the test function[2]. The computer programming guidelines supplied by Moore and Zeigler[3] were followed. A statistical weight $1/N$ was assigned to the datum N - this weighting formula is appropriate for data in which $\sqrt{N}$ noise is expected.

Having dispatched the most general aspects of the linewidth analysis problem, we devote the remainder of this chapter to those aspects peculiar to the experiments on which the present work is based.

Separation Of Reorientational From Other Broadening Mechanisms

To this point, we have blithely alluded to the spectrum we propose to fit, as though it were directly available from the experimental data. Such is, regrettably, not the case for the reorientational spectrum.

Rather, as shown in III. of Ch. 2 via the assumptions that

(a) reorientational and non-reorientational processes contributing to the spectral broadening are statistically independent, and

(b) non-reorientational processes contribute equally to the isotropic and anisotropic spectra,

the anisotropic spectrum represents the convolution of the reorientational and isotropic spectra:

$$I_{anis} \sim I_{iso} * I_{or} .$$

Within the restriction, already agreed upon, to analysis in the frequency domain, two possible methods emerge, by which one may extract correlation times from the data:

(1) If it is assumed that <u>both</u> I_{iso} and I_{or} are Lorentzian, then their convolution I_{anis} - which the data yield directly by (2.5) - is again Lorentzian, with a half-width equal to the sum of half-widths of I_{iso} and I_{or} . The reorientational correlation time

$$\tau_{or} \sim 1/\Gamma_{or} = 1/(\Gamma_{anis} - \Gamma_{iso})$$

is thus determined, once I_{iso} and I_{anis} have been separately fit to Lorentzians of width Γ_{iso} and Γ_{anis} respectively. This method has been applied with some success in various Raman linewidth studies[4,5] . It enjoys the advantages of simplicity and economy in data processing. Its validity is restricted, however, by the required assumption that I_{iso} is Lorentzian; also, the results for Γ_{or} are subject to instrumental correction.

(2) An alternative method, directly suggested by the relation $I_{anis} \sim I_{iso} * I_{or}$, is to deconvolute I_{iso} from I_{anis} , thus recovering

I_{or} , and to fit the latter to a Lorentzian. The correlation time is then given directly by

$$\tau_{or} \sim 1 / \Gamma_{or} \ .$$

This method is in principle more general and more accurate than method (1), since it obviates both the need for the assumption that I_{iso} is Lorentzian, and, as will be seen presently, the need for explicit instrumental correction. Owing to the inherent messiness of deconvolution procedures, however, it takes its toll in computer time.

Both of the above methods were pursued. The difficulties encountered, and the techniques brought to bear on them, will be elaborated below in considerable detail. All points discussed with reference to method (1) (under I.), save that of instrumental correction, are relevant also to method (2). Even the latter point is of some importance in (2), inasmuch as one and the same method has been used for instrumental correction in (1), and for deconvolution in (2): only the purpose, not the method, differs. Considerations peculiar to method (2) are discussed under II. For both methods, $I_{\parallel}$ was used in place of I_{iso} , without correction, in all calculations. The strong polarisation of the benzene 992 $cm.^{-1}$ line, rendered negligible the difference between the two spectra. As indicated by our prefatory remarks, method (2) met with much greater success than did method (1), for reasons yet unclear to the author.

I. <u>Method (1) - Separate Fitting of I_{anis} and I_{iso} to Lorentzian:</u>

The problems to be dealt with here are that of instrumental distortion of the spectrum, and that of the entry of stray, isotropically scattered light into the depolarised spectrum. A general approach to the removal of such effects was adopted, consisting in the introduction

of corresponding modifications to the test function against which the (uncorrected) data were fit. By this means, such corrections can be incorporated neatly within the usual least-squares fitting procedure.

A. The Problem of Instrumental Distortion:

The observed spectrum may be taken as a convolution of the true spectrum, with an "instrumental profile" $S(\omega)$ describing the distribution in measured frequency, of unit intensity of light unaffected by passage through the sample. In the present work, the instrumental broadening is essentially just the "slit broadening" of the spectrometer. It would not matter in principle, however, if, say, the finite width of the laser line contributed appreciably to the instrumental broadening. The profile $S(\omega)$ is directly measurable; in fact, the measurement described in B.1. of Ch. 3 was just that of $S(\omega)$, since the process of Tyndall scattering has no effect on the frequency distribution of light.

The true spectrum can, in principle, be recovered by deconvolution when $S(\omega)$ is known. We proceed to survey several current methods to this end, before discussing the method that was actually used.

1. Zero Slit-width Extrapolation:

A purist's solution, which obviates deconvolution altogether, is the "ZSE" method advocated by Griffiths[6]. This involves measuring the widths of the instrumentally broadened spectra at a series of progressively narrower slit-widths, then extrapolating these measurements to zero slit-width. The method may be suspected of systematically overestimating linewidths by, perhaps, 4 $cm.^{-1}$, because, even in the limit of zero slit-width, there remains some instrumental broadening due to the diffraction limit of the spectrometer and to the finite width of the laser line. The loss of signal strength at low slit-widths, moreover, would prove

prohibitive in the present work, where weak depolarised scattering from a dilute solution must be measured. In any case, a recent investigation[7] indicates that deconvolution can reproduce consistently the results obtained via ZSE.

2. Integral Transform Deconvolution Methods:

Deconvolution is usually accomplished by Fourier or Laplace transform methods[8] - e.g., the Rakov - Sykora algorithm. These are not, however, always easy to apply, since:

(a) The unfolded curve tends to show unphysical oscillations because of statistical uncertainty in the data points.[9]

(b) The solution is not unique - it is inherently underdetermined, because the folded data at the ends of the specified interval inevitably depend on values of the unfolded curve outside the specified interval.

3. Voigt Profiles:

Methods have recently been suggested[9,10,11] for fitting of Voigt functions to Raman lines. A Voigt function, which is the convolution of a Gaussian with a Lorentzian, may be a good approximation to the observed Raman line, since in the diffraction (narrow slit) limit, the slit function of a modern monochromator is closely Gaussian. Upon fitting a Voigt function to the Raman profile, one obtains separate estimates for the widths of the Gaussian and Lorentzian components of the profile, which may be identified respectively with the slit-width and the true Raman linewidth, if the slit function is well approximated by a Gaussian. In the present work, however, the slit-widths used were broad enough so that the slit functions were not Gaussian, but more or less triangular. Occasionally, in fact, they were visibly asymmetric, owing to alignment imperfections. They were, in any case, analytically nondescript.

So Voigt profiles were judged insufficient to the task.

All these approaches to instrumental correction were rejected for various reasons cited above. In their stead, a method of deconvolution was developed which, as has been indicated above, basically involves a modification of the test function to which the data are fit.

The Deconvolution Procedure:

The method employed in the present work differs from the usual (Fourier) deconvolution procedure, in that no attempt is made to solve the unfolded spectrum point-by-point.

Ordinarily, deconvolution entails the generation of a new set of "corrected" data from the raw data, without reference to any particular class of test function to describe the spectrum. It is in the attempt to correct each datum individually, that the problem of underdetermination arises. If we represent the convolution S*X of the instrumental profile S with the spectrum X as a Riemann sum, then our knowledge of the spectrum is expressible in terms of the data Y as follows:

$$\sum_{i=1}^{w} s_i \; x_{k-i} = y_k \quad , \quad k = 1,\ldots,n.$$

The n data supply n equations, but these involve n+w-1 unknown x-values, and are thus underdetermined for a "slit-width" $w > 1$.

In the present work, however, it is unnecessary to solve for the individual x_j . Our interest is confined to a few lineshape parameters that optimise their congruence to a particular sort of test function. One might, indeed, explicitly deconvolute the data - and then effectually discard most of the resulting hard-gotten information by fitting the deconvoluted spectrum to a test function, and using only the optimal

parameter values. The task may be considerably simplified, however, if one aims in the first place only to solve the parameter values; one then deals with a vastly reduced set of unknowns. The means by which this was accomplished, are explained below.

To solve the optimal parameter values -

The process of correcting the optimal parameter values for instrumental effects was incorporated directly within the least-squares fitting routine. The convolution of the lineshape with the instrumental profile S was simply absorbed into the form of test function to which the data were compared in the course of the fit. If $F(x; \{a_1,\ldots,a_p\})$, a function of frequency x and of a set of adjustable parameters $\{a_1,\ldots,a_p\}$, were the analytical form expected to represent the true lineshape (i.e., a Lorentzian plus a constant background), then the test function would become

$$T(x) = S*F = \int_{-c}^{c} dx'\ S(x')\ F(x-x'; \{a_1,\ldots,a_p\}), \qquad \ldots(4.1)$$

where the instrumental profile S(x') has been truncated to lie within the finite interval (-c,c). The set $\{\bar{a}_1,\ldots,\bar{a}_p\}$ of parameter values which produces the best agreement between T(x) and the data, yields the best estimate $F(x; \{\bar{a}_1,\ldots,\bar{a}_p\})$ for the true (unfolded) lineshape.

It remains to verify that T(x) is amenable to the usual least-squares analysis. When this is carried out, as in the present work, by linearisation of the test function, a set of initial estimates $\{a_1^o,\ldots,a_p^o\}$ for the best parameter values is improved upon by adding a set of parameter increments $\{\delta a_1,\ldots,\delta a_p\}$, which are solutions to

the following set of linear "normal equations"[2]:

$$\sum_{i=1}^{n} w_i \left[y_i - T(x_i) \right] \frac{\partial T(x_i)}{\partial a_j} \Big|_{\{a_1,\ldots,a_p\}=\{a_1^\circ,\ldots,a_p^\circ\}}$$

$$= \sum_{k=1}^{p} \delta a_k \left[\sum_{i=1}^{n} w_i \frac{\partial T(x_i)}{\partial a_j} \frac{\partial T(x_i)}{\partial a_k} \right] \Big|_{\{a_1,\ldots,a_p\}=\{a_1^\circ,\ldots,a_p^\circ\}} \quad , j = 1,\ldots,p \ ,$$

where the ordered pairs $(x_1, y_1), \ldots, (x_n, y_n)$ are the data, and where w_i is the statistical weight associated with y_i. This procedure is then repeated, with the improved estimates

$$\{a_1^1, \ldots, a_p^1\} = \{a_1^\circ + \delta a_1, \ldots, a_p^\circ + \delta a_p\}$$

replacing $\{a_1^\circ, \ldots, a_p^\circ\}$. One continues in this fashion until the estimates converge.

It is evident from the form of the normal equations, that any test function T may be used, so long as T and its parametric derivatives $\partial T / \partial a_j$ are explicitly calculable. The form of T proposed in (4.1) above satisfies these conditions: T(x) may be calculated numerically as a Riemann sum, since S is known experimentally and F is an analytical form; the derivatives

$$\partial T(x)/\partial a_j = \int_{-c}^{c} dx' S(x') \frac{\partial}{\partial a_j} F(x-x'; \{a_1, \ldots, a_p\})$$

may be calculated likewise. Thus, even though T is not an analytical form, it is perfectly serviceable as a least-squares test function.

Apologia -

The merits of the above approach to instrumental correction, are:

(a) The method is simple, requiring only minor modifications to an

operational non-linear least-squares computer program.

(b) The amount of data processing is minimized, in that instrumental correction and fitting are carried out in the same operation.

(c) The problem of underdetermination is eliminated. Thus, no new convergence problems arise that were not inherent in the iterative least-squares fitting procedure.

(d) The instrumental profile S need only be known empirically; it does not have to be approximated by any particular analytical form.

The obvious limitation is that the actual unfolded spectrum is not recovered, only its best fit to the particular model F. The quality of the information acquired thus depends on a felicitous choice of model.

The subtle limitation is that meaningful fits can be expected only if the function F is a good model, not only in the data interval over which the fit is performed, but also, as far beyond the edges as S overlaps. In practice, however, this poses a problem only if there are strong peripheral structures in the neighbourhood of the spectral line of interest.

The test function of (4.1) was adequate for the fitting of polarised spectra, and hence for the determination of Γ_{iso}. Further elaboration of T(x) was required, however, before the depolarised spectra could be treated, since the analysis of these spectra had to compensate for stray light as well as for instrumental distortion.

B. The Problem Of Stray Light:

Because of the strong polarisation of the 992 $cm.^{-1}$ benzene line, experimental precautions alone did not suffice to isolate the isotropic scattering component from the depolarised spectra. Accordingly, a

correction was undertaken in the analysis. In the same spirit that informed the instrumental correction discussed above, this was accomplished by a further modification of the test function to which the depolarised data were fit. This became,

$$T_{\perp}(x) = S*F_{\perp}(x;\{a_1,\ldots,a_p\}) + cI_{\parallel}(x), \qquad \ldots(4.2)$$

where $I_{\parallel}$ is the measured polarised spectrum, and c is a new parameter, subject to least-squares optimisation along with the a_j . (The new term remains outside the convolution, since the measured form of $I_{\parallel}$ is already instrumentally distorted.) The problem can still be handled by least-squares: $T_{\perp}$ is computable, since $I_{\parallel}$ is known experimentally; $\partial T_{\perp}/\partial a_j$ is as before; $\partial T_{\perp}/\partial c = I_{\parallel}$ is known experimentally.

Treating c as a least-squares parameter, one avoids the several drawbacks, mentioned in B.4. of Ch. 3, of making a single experimental measurement of c. The calculated value of c no longer depends on any physical constants, such as the depolarisation ratio used in B.4 of Ch. 3, which might limit the accuracy of the calculation. There is no need to correct c for the change in grating efficiency with change of polarisation. Legitimate variations in the value that c might assume at different temperatures or for different liquids, because of index of refraction effects, etc., are no longer a matter of concern, since a separate determination of c is made for each new spectrum. Finally, an important implication to the conduct of the experiment, is that the requirements for the maintenance, between polarised and depolarised scans, of optical alignments, laser power, and anything else that affects the intensity of the spectrum, are somewhat relaxed. One may, between scans, focus the optics, adjust the laser output, insert

neutral density filters, and change scanning rates with gay abandon, without having to adjust the value of c explicitly. All these liberties were exercised in the course of the experiment.

Some a posteriori justification for leaving c as a free parameter, as opposed to fixing its value, emerged from the results of the fits, which showed a strong tendency for c to rise as temperature dropped.

One limitation of the method is that it would break down if the isotropic and anisotropic lineshapes were closely similar. This is because c is determined by resolving the measured depolarised spectrum into a linear combination of $(S*F_{\perp})$ and of $I_{\parallel}$, the coefficients of which cannot be specified definitively if the basis functions $(S*F_{\perp})$ and $I_{\parallel}$ resemble each other too closely. But this would occur only if Γ_{or} were small in comparison to Γ_{iso}, in which case Γ_{or} could not be determined accurately, even in the absence of stray light.

Correction for frequency mismatch between polarised and depolarised spectra -

It is implicit in the foregoing discussion, that in correcting the depolarised spectrum for stray light, one must superpose the polarised spectrum on the depolarised in such a manner that data of identical light frequencies are matched together. This requirement posed a problem, for the two spectra were taken during separate scans of the spectrometer, and it was found (cf. B.3. of Ch. 3) that the indicated frequency, at which a given actual frequency would be read out, was not perfectly reproducible between scans. Computer experiments revealed that the results of the fit, when (4.2) was used for the test function, were quite sensitive to a deliberate shifting of one data field relative to the other, even by .2 $cm.^{-1}$, so that this consideration proved quite critical.

One means that was contemplated to circumvent this difficulty,

was simply to match together the peaks of the two spectra. Uncertainties in the peak positions, due to statistical fluctuations in the data around the peak, could be suppressed by taking as the peak the centroid of, say, that part of the spectrum above half-maximum. It is not certain, however, that the actual frequencies of the two peaks coincide exactly. Some evidence has been reported[5] of a physical frequency shift between polarised and depolarised peaks in liquid phosphine. Without a priori knowledge of whether such a phenomenon occurs in benzene, this peak-matching procedure would seem ill-advised.

A method of correction was devised, which followed in the same vein as the corrections which have already been discussed: a further modification of the test function, involving a new least-squares parameter, was introduced. The term $cI_{\parallel}(x)$ in the test function (4.2) was replaced by its translate along the x-axis. The test function became

$$T_{\perp}(x) = S*F_{\perp}(x; \{a_1,\ldots,a_p\}) + cI_{\parallel}(x+b) , \qquad \ldots (4.3)$$

where b is a new parameter, subject to least-squares optimisation, representing the amount by which one data field has been shifted relative to the other. A minor annoyance was that the digitally recorded data were taken only at discrete x-values, and (x+b) would generally fall between two such values. Accordingly, $I_{\parallel}(x+b)$ was defined by linear interpolation between the two data channels bracketing (x+b). The computability of $T_{\perp}(x)$ was thus preserved. By the same token, linear interpolation of $I_{\parallel}$ between channels yielded a presciption for the parametric derivative $\partial T_{\perp}/\partial b$:

$$\frac{\partial T_{\perp}(x)}{\partial b} = c\,\frac{\partial}{\partial(x+b)}\,I_{\parallel}(x+b) \rightarrow c\,\frac{I_{\parallel}(x_{i+1}) - I_{\parallel}(x_i)}{x_{i+1} - x_i} ,$$

where x_i and x_{i+1} are the data channels bracketing (x+b). Moreover, $\partial T_\perp(x)/\partial c = I_{\parallel}(x+b)$, and $\partial T_\perp/\partial a_j$ is as before. Thus, $T_\perp(x)$ and all its parametric derivatives are calculable, and $T_\perp(x)$ remains a valid least-squares test function.

The results of fits to the test function (4.3), indicated a systematic bias of perhaps .5 $cm.^{-1}$ in the optimised b-values, from the expected value of zero, and a comparable amount of scatter. The bias might be due to an optical wedge effect associated with rotation of the polarisation analyser, which could shift the frequency calibration of the spectrometer. The random component might arise from mechanical backlash in the grating drive of the spectrometer, which could render the frequency calibration imperfectly reproducible on different scans. Some uncertainty lingers, however, as to the origin of this frequency mismatch.

One might understandably incline toward skepticism of the validity of introducing new parameters to the test function in, as it were, an ad hoc manner. Any resulting success in improving the quality of the fit, as measured by the value of χ^2, may be challenged on the basis that adding a new parameter, whether or not it has genuine physical significance, will inevitably improve the fit, just by augmenting the degrees of freedom available to the test function.

A case can be made, however, that the non-zero values of b which were obtained, are not merely an artifact of the fit. Before the parameter b was introduced - that is, when b was effectively set to zero - the fit results, with (4.2) as the test function, were typified by those illustrated in Fig. 4. It is evident from the figure, that there are intervals in which the fit departs significantly from the data.

FIG. 4

Illustration of the failure of test function (4.2).

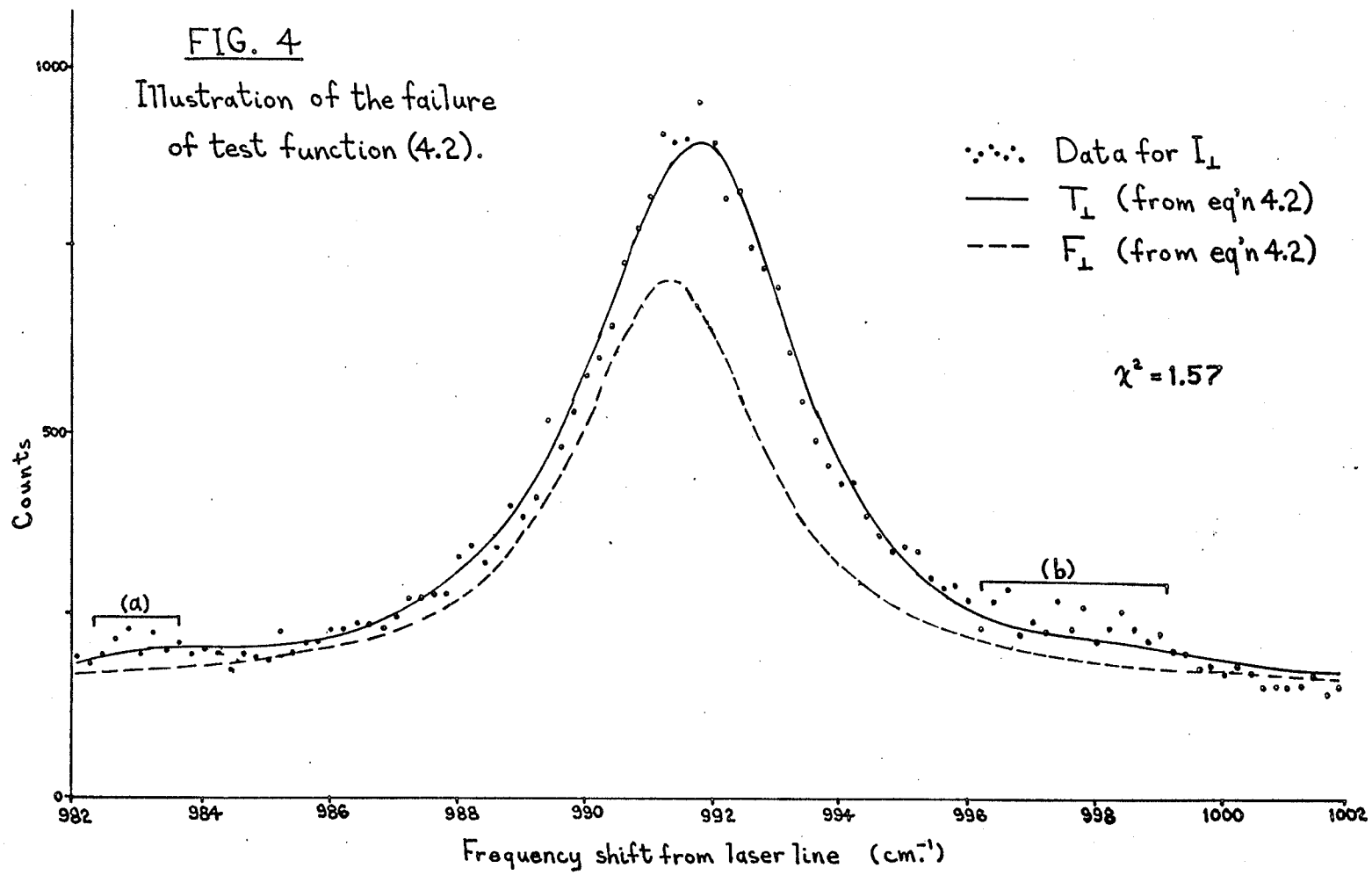

Also apparent is a discrepancy between the data peak, and the position assigned by the fit to the peak of $F_\perp$ (not to be confused with a shift between the peaks of $I_\parallel$ and $I_\perp$, which, as mentioned earlier, might be physical in origin). These features are accountable in terms of a spurious frequency shift between the records of $I_\perp$ and $I_\parallel$. Such a shift could be expected to reduce the fit value of c from its true value, since the fit would scarcely be improved by adding the full measure of $I_\parallel$ in the wrong part of the depolarised spectrum. A reduction in c would tend unduly to suppress peripheral structures - the isotope-shifted peak (a) on the left of Fig. 4, and the hot-band shoulder (b) on the right - which are prominent in the polarised spectrum, but which are diffused by reorientational broadening in the depolarised, and thus appear in the measurement of the latter mainly through stray light. This expectation is in harmony with the observation that the fit falls beneath the data in regions (a) and (b). Moreover, the displacement of $F_\perp$ to the left, can be interpreted as the way in which the fit should respond to a spurious shift of $I_\parallel$ to the right: since the term $cI_\parallel$ in the test function would be too high on the right and too low on the left of the peak region, the fit would compensate by making $F_\perp$ too low on the right and too high on the left - i.e., by shifting $F_\perp$ to the left. When b was introduced as a free parameter, the fit results for this same set of data were as illustrated in Fig. 5. It is evident that the most egregious features of the first fit have been eliminated. The positive value obtained for b is consistent with the above supposition that $I_\parallel$ is shifted to the right.

II. <u>Method (2) - Recovery of I_{or} by Deconvolution of I_{iso} from I_{anis}</u>:

The method discussed in I. requires separate fits to be performed

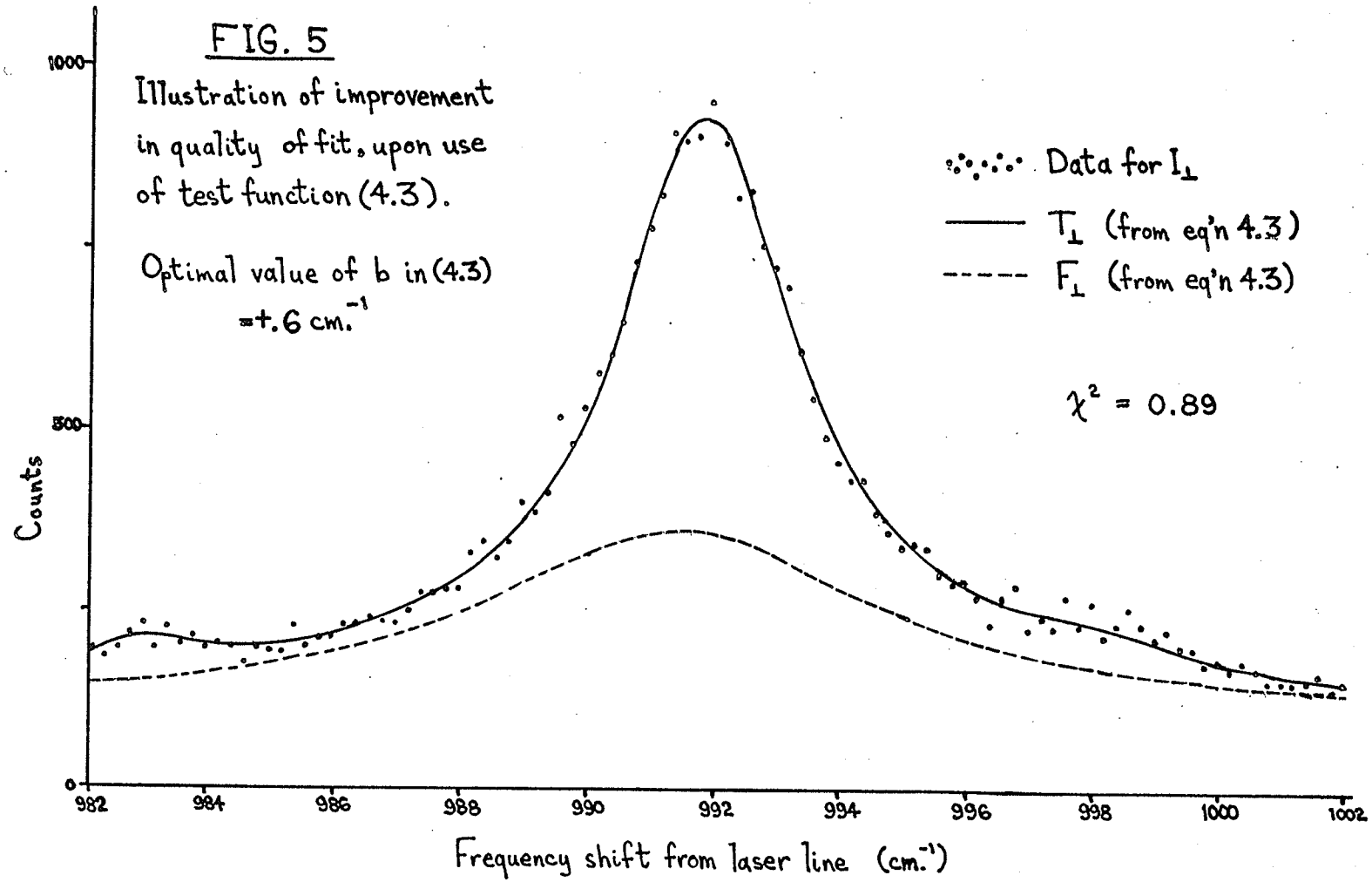
FIG. 5
Illustration of improvement in quality of fit, upon use of test function (4.3).
Optimal value of b in (4.3) = +.6 cm.$^{-1}$
Data for $I_\perp$
$T_\perp$ (from eq'n 4.3)
$F_\perp$ (from eq'n 4.3)
$\chi^2 = 0.89$
Counts
1000
500
0
982
984
986
988
990
992
994
996
998
1000
1002
Frequency shift from laser line (cm.$^{-1}$)

on the polarised and depolarised spectra, before Γ_{or} may be calculated. By contrast, the present method permits a determination of Γ_{or} in the course of fitting just the depolarised spectrum. The other salient difference between the two methods, is that the present method requires no explicit correction to be made for instrumental effects, provided that the instrumental profile S is the same for both the polarised and the depolarised spectrum. (This was ensured in the experiment by using the same slit width for both spectra.) Stray light, however, was dealt with identically by the two methods.

The test function to be applied to the depolarised spectrum, develops as follows. It will be recalled that the anisotropic spectrum takes the form

$$I_{anis} \sim I_{iso} * I_{or} ,$$

so that its measurement, through an instrument with transfer function S, takes the form

$$S*I_{anis} \sim S* (I_{iso} *I_{or}).$$

Because convolution is associative, this may be written

$$S*I_{anis} \sim (S*I_{iso}) * I_{or} .$$

On the assumption that S is the appropriate instrumental profile for the polarised, as well as the depolarised spectrum, $(S*I_{iso})$ may be identified as the measurement $I_{\parallel}$ of the polarised spectrum (insofar as, for a strongly polarised line, one may ignore the small anisotropic

contribution to $I_{\parallel}$). Hence,

$$S*I_{anis} \sim I_{\parallel} * I_{or} \quad .$$

With the inclusion of stray light, which enters in the same manner as in I., the measured form of the depolarised spectrum becomes

$$I_{\parallel} * I_{or} (x) + cI_{\parallel}(x+b).$$

When a particular analytical form F_{or} $(x;\{a_1,\ldots,a_p\})$ (viz., a Lorentzian plus horizontal background) is substituted for I_{or} , one obtains, in analogy to (4.3), the following test function against which to fit the depolarised spectrum:

$$T_{\perp}(x) = I_{\parallel} *F_{or} (x;\{a_1,\ldots,a_p\}) + cI_{\parallel} (x+b) \quad \ldots(4.4)$$

Since $I_{\parallel}$ is known experimentally, and since (4.3) and (4.4) are formally identical, the fitting problem is the same one encountered in I., except that $I_{\parallel}$ replaces S. (S no longer appears explicitly in the test function, because it is subsumed in $I_{\parallel}$.) Accordingly, the same deconvolution method which was developed in I.A. to extract $F_{\perp}$ from its convolution with S, may again be applied, this time to extract F_{or} from its convolution with $I_{\parallel}$. In the present case, the solution F_{or} $(x; \{\bar{a}_1,\ldots,\bar{a}_p\})$ of the least-squares problem represents I_{or} directly, whereas the solution $F_{\perp}$ in I. represented I_{anis} . Thus, no further calculations are required to determine Γ_{or} .

The method just described is more general than that of I., in that no special assumptions are made in regard to the isotropic lineshape. Peripheral structure in the lineshape therefore presents less of a problem. Certain limitations, however, ought still to be observed.

The assumption is required[12], that all structures within the line shape have the same depolarisation ratio. While this may be well satisfied if the peripheral structure consists, say, in a hot band, it may be quite inappropriate if the structure arises from the overlap of neighbouring lines corresponding to different vibrational modes.

In actual calculations, the polarised spectrum must, of course, be truncated to lie within some finite interval. In principle, the broader, the better. In practice, the breadth of interval was decided on the basis of computer experiments, in which the interval was progressively broadened until the fit values of Γ_{or} converged. The interval settled upon was just slightly less broad than the depolarised data interval over which the fit was performed. This interval was, of course, much broader than the slit function. For this reason, the present method was found to devour much more computer time than the method of I.

References:

1. R. B. Wright, M. Schwartz, and C. H. Wang, J. Chem. Phys. 58, 5125 (1973).
2. P. R. Bevington, "Data Reduction and Error Analysis for the Physical Sciences" (McGraw-Hill, Inc., New York, 1969), pp. 232-237.
3. R. H. Moore and R. K. Zeigler, LASL Report LA-2367, (Office of Technical Services, Dept. of Commerce, 1960).
4. J. E. Griffiths, J. Chem. Phys. 59, 751 (1973).
5. M. Schwartz and C. H. Wang, Chem. Phys. Letters 25, 26 (1974).
6. K. T. Gillen and J. E. Griffiths, Chem. Phys. Letters 17, 359 (1972).
7. F. G. Baglin, R. B. Thomas, and G. N. Fickes, J. Chem. Phys. 60, 2475 (1974).
8. J. E. Stewart, "Infrared Spectroscopy" (Marcel Dekker, Inc., New York, 1970), p. 461.
9. T. Sundius, J. Raman Spectry. 1, 471 (1973).
10. J. F. Kielkopf, J. Opt. Soc. Am. 63, 987 (1973).
11. G. K. Wertheim, M. A. Butler, K. W. West, and D.N.E. Buchanan, Rev. Sci. Instrum. 45, 1369 (1974).
12. F. J. Bartoli and T. A. Litovitz, J. Chem. Phys. 56, 404 (1972).

CHAPTER 5

RESULTS OF LINEWIDTH ANALYSIS

Here we present the results of our linewidth analysis. All widths quoted are full widths at half-maximum (FWHM). The error quoted for each linewidth, is the larger of the internal and external errors [1], the former being the error propagating from the statistical uncertainty in the individual spectral data, and the latter being determined by the degree of "external consistency" of the body of data with the form of test function to which it is fit.

In Table 1. appear the results of analysis by Method (1), outlined in I. of Ch. 4. The reorientational linewidths were obtained from the relation

$$\Gamma_{or} = \Gamma_{anis} - \Gamma_{iso} \quad ,$$

as discussed in Ch. 4. The correlation times and diffusion constants were thereupon derived, respectively, from

$$\tau_{or} = (\pi c \Gamma_{or})^{-1} \qquad \ldots (2.22)$$

and

$$D_{\perp} = \frac{\pi c}{6} \Gamma_{or} \, . \qquad \ldots (2.23b)$$

In the instance where a comparison with literature values is possible - for pure benzene at room temperature - our Method (1) result for Γ_{or} significantly exceeds those quoted by Gillen and Griffiths[2], and by Bartoli and Litovitz[3]. (The former authors find $\Gamma_{or} = 3.8$ cm.$^{-1}$ through separate fitting of the polarised and depolarised spectra to Lorentzians, as in our Method (1); the latter authors obtain $\Gamma_{or} = 4.0 \pm 1.0$ cm.$^{-1}$ by deconvolution of the polarised from the

depolarised spectrum, as in our Method (2).) The discrepancy persisted over numerous repetitions of the experiment. Therefore, we shall base no further results on calculations using Method (1) values of Γ_{or}.

Reference will be made, however, to the isotropic linewidths shown in Table 1., in the discussion (Ch. 7) of vibrational relaxation. These linewidths were computed by fitting only on the structure-free side of the polarised spectrum: there is a hot band on the high-frequency-shift side, which would preternaturally broaden the linewidth estimate if included. It is worth noting that the broadening effect of the hot band on the depolarised spectrum was uncompensated in Method (1), while the effect was removed from the polarised spectrum. This uneven treatment of the two spectra may be partially responsible for the aforementioned error in the determination of Γ_{or}. It has been reported[4], however, that the hot band, if not removed, contributes only about .2 $cm.^{-1}$ to the total observed polarised bandwidth. Our observations are consistent with this. The effect of our treatment of the hot band, is therefore quantitatively inadequate to explain the discrepancy.

The results of analysis by Method (2), which was outlined in II. of Ch. 4, are presented in Table 2. Correlation times and diffusion constants were again derived from (2.22) and (2.23b). These results are used in the further calculations that arise in the discussion (Ch. 6) of reorientational motion.

References:

1. R. T. Birge, Phys. Rev. 40, 207 (1932).

2. K. T. Gillen and J. E. Griffiths, Chem. Phys. Letters 17, 359 (1972).

3. F. J. Bartoli and T. A. Litovitz, J. Chem. Phys. 56, 404 (1972).

4. J. E. Griffiths, M. Clerc, and P. M. Rentzepis, J. Chem. Phys. 60, 3824 (1974).

TABLE 1.

Results of Method (1) Analysis.

TEMP. (°K.)	Γ_{anis} ($cm.^{-1}$)	Γ_{iso} ($cm.^{-1}$)	Γ_{or} ($cm.^{-1}$)	τ_{or} (psec.)	$10^{-10} \times D_{\perp}$ ($sec.^{-1}$)
Mixture #1: f_B^*= 1.00 , f_C^*= 0.00 (pure benzene)					
295	6.84±.44	1.79±.04	5.06±.44	2.1±.2	8.0±.7
295	7.74±.48	1.68±.04	6.06±.48	1.8±.2	9.5±.8
291	7.02±.46	1.92±.03	5.10±.46	2.1±.2	8.0±.7
287	6.62±.44	1.92±.03	4.70±.44	2.3±.2	7.4±.7
283	7.74±.50	2.02±.02	5.72±.50	1.9±.2	9.0±.8
280	6.96±.40	1.98±.03	4.98±.40	2.1±.2	7.8±.6
279	6.46±.44	2.06±.02	4.40±.44	2.4±.2	6.9±.7
279	6.24±.44	2.02±.02	4.22±.44	2.5±.3	6.6±.7
Mixture #2: f_B= .81 , f_C = .19					
295	7.12±.42	1.56±.06	5.56±.42	1.9±.2	8.7±.7
295	6.52±.40	1.59±.06	4.92±.40	2.2±.2	7.7±.6
290	6.42±.36	1.63±.06	4.78±.36	2.2±.2	7.5±.6
286	7.06±.50	1.57±.04	5.50±.50	1.9±.2	8.6±.8
282	6.38±.42	1.65±.04	4.74±.42	2.2±.2	7.5±.7
277	6.52±.44	1.68±.03	4.84±.44	2.2±.2	7.6±.7
273	6.92±.54	1.67±.03	5.26±.54	2.0±.2	8.3±.9
269	5.36±.32	1.69±.03	3.66±.32	2.9±.3	5.8±.5
267	5.78±.34	1.70±.03	4.08±.34	2.6±.2	6.4±.5
Mixture #3: f_B= .62 , f_C =.38					
295	6.68±.48	1.67±.03	5.02±.48	2.1±.2	7.9±.8
295	7.16±.62	1.69±.03	5.48±.62	1.9±.2	8.6±1.0
288	6.54±.42	1.78±.02	4.78±.42	2.2±.2	7.5±.7
281	6.04±.50	1.64±.03	4.40±.50	2.4±.3	6.9±.8
275	6.48±.48	1.63±.03	4.86±.48	2.2±.2	7.6±.8
269	5.66±.42	1.70±.03	3.96±.42	2.7±.3	6.2±.7
266	5.26±.38	1.72±.03	3.54±.38	3.03±.3	5.6±.6

*$f_B \equiv$ mole fraction of benzene in mixture; $f_C \equiv$ mole fraction of carbon tetrachloride.

TABLE 1. (Cont'd)

TEMP. (°K.)	Γ_{anis} (cm^{-1})	Γ_{iso} (cm^{-1})	Γ_{or} (cm^{-1})	τ_{or} (psec.)	$10^{-10} \times D_{\perp}$ (sec^{-1})
Mixture #4: f_B =.42 , f_C =.58					
295	6.16±.60	1.46±.04	4.70±.60	2.3±.3	7.4±.9
295	6.62±.56	1.48±.04	5.14±.56	2.1±.2	8.1±.9
288	6.86±.70	1.50±.04	5.36±.70	2.0±.3	8.4±1.1
288	7.46±.68	1.46±.04	6.00±.68	1.8±.2	9.4±1.1
281	7.10±.62	1.47±.02	5.62±.62	1.9±.2	8.8±1.0
275	5.76±.44	1.62±.02	4.14±.44	2.6±.3	6.5±.7
275	5.86±.54	1.58±.03	4.28±.54	2.5±.3	6.7±.9
269	6.50±.58	1.62±.03	4.88±.58	2.2±.3	7.7±.9
263	6.20±.54	1.62±.03	4.58±.54	2.3±.3	7.2±.9
263	6.60±.64	1.68±.04	4.92±.64	2.2±.3	7.7±1.0
258	5.76±.52	1.65±.04	4.12±.52	2.6±.3	6.5±.8
258	6.20±.56	1.69±.05	4.52±.56	2.3±.3	7.1±.9
Mixture #5: f_B =.21 , f_C =.79					
295	7.92±.94	1.20±.04	6.72±.94	1.6±.2	10.6±1.5
295	7.40±.50	1.20±.03	6.20±.50	1.7±.1	9.7±.8
288	7.24±.50	1.25±.03	5.98±.50	1.8±.2	9.4±.8
281	6.98±.44	1.22±.03	5.76±.44	1.8±.1	9.0±.7
274	6.54±.44	1.27±.03	5.28±.44	2.0±.2	8.3±.7
266	5.60±.40	0.73±.06	4.88±.40	2.2±.2	7.7±.6
260	6.06±.40	0.69±.05	5.36±.40	2.0±.2	8.4±.6
252	5.78±.48	0.64±.06	5.14±.48	2.1±.2	8.1±.8

TABLE 2

Results of Method (2) Analysis.

TEMP. (°K.)	Γ_{or} (cm^{-1})	τ_{or} (psec.)	$10^{-10} \times D_{\perp}$ (sec^{-1})
Mixture #1: f_B*=1.00, f_C*=0.00 (pure benzene)			
295	4.34±.46	2.44±.26	6.82±.72
295	4.16±.48	2.55±.29	6.53±.75
291	4.00±.42	2.65±.28	6.28±.66
287	4.12±.60	2.58±.38	6.47±.94
283	4.84±.68	2.19±.31	7.60±1.07
280	3.78±.50	2.81±.37	5.94±.79
279	2.68±.48	3.96±.71	4.21±.75
279	3.02±.44	3.51±.51	4.74±.69
Mixture #2: f_B=.81 , f_C=.19			
295	4.26±.50	2.49±.29	6.69±.79
295	4.20±.42	2.53±.25	6.60±.66
290	3.70±.42	2.87±.33	5.81±.66
286	4.08±.56	2.60±.36	6.41±.88
282	3.56±.46	2.98±.39	5.59±.72
277	4.04±.41	2.63±.27	6.35±.64
273	3.62±.54	2.93±.44	5.69±.84
269	2.82±.40	3.76±.53	4.43±.63
267	3.34±.40	3.18±.38	5.25±.63
Mixture #3: f_B=.62 , f_C=.38			
295	4.38±.76	2.42±.42	6.88±1.19
295	3.08±.48	3.44±.54	4.84±.75
288	3.76±.48	2.82±.36	5.91±.75
281	3.18±.66	3.34±.69	5.00±1.04
275	3.60±.48	2.95±.39	5.65±.75
269	3.36±.44	3.16±.41	5.28±.69
266	3.02±.50	3.51±.58	4.74±.79

*$f_B \equiv$ mole fraction of benzene in mixture; $f_C \equiv$ mole fraction of carbon tetrachloride.

TABLE 2 (Cont'd)

TEMP. (°K.)	Γ_{or} ($cm.^{-1}$)	τ_{or} (psec.)	$10^{-10} \times D_{\perp}$ ($sec.^{-1}$)
Mixture #4: f_B=.42, f_C=.58			
295	3.88±68	2.73±.48	6.09±1.07
295	3.68±.36	2.88±.28	5.78±.57
288	4.04±.86	2.63±.56	6.35±1.35
288	3.84±.74	2.76±.53	6.03±1.16
281	4.08±.92	2.60±.59	6.41±1.45
275	3.40±.54	3.12±.50	5.34±.85
275	3.50±.48	3.03±.42	5.50±.75
269	3.44±.54	3.08±.48	5.40±.85
263	3.52±.52	3.01±.45	5.53±.82
263	4.38±.70	2.42±.39	6.88±1.10
258	3.78±.56	2.81±.42	5.94±.88
258	3.72±.54	2.85±.41	5.84±.85
Mixture #5: f_B=.21, f_C =.79			
295	4.14±.84	2.56±.52	6.50±1.32
295	4.90±.56	2.17±.25	7.70±.88
288	4.92±.60	2.16±.26	7.73±.94
281	4.98±.54	2.13±.23	7.82±.85
274	4.18±.52	2.54±.32	6.57±.82
266	3.22±.44	3.30±.45	5.06±.69
260	4.16±.44	2.55±.27	6.53±.69
252	4.56±.64	2.33±.33	7.16±1.01

CHAPTER 6

DISCUSSION - REORIENTATIONAL MOTION

Within the scope of this chapter falls any information which was obtained from the lineshapes and linewidths of the reorientational spectra. In particular, we shall investigate the validity of the rotational diffusion model proposed in IV. of Ch. 2, as a description of the tumbling motion of the benzene molecule about axes perpendicular to the symmetry axis.

It was seen in IV. of Ch. 2, how a rotational Brownian motion model, in the diffusion limit, leads to a Lorentzian lineshape for the reorientational spectrum. The experimental observation of Lorentzian lineshapes is, then, at least consistent with such a diffusive mechanism. By no means, however, does this observation unequivocally corroborate the model in question. Other, quite different reorientation models have been propounded which likewise predict Lorentzian lineshapes. An example is the van Vleck-Weisskopf collision-broadening theory[1], which postulates that molecules rotate freely between instantaneous collisions, but that each collision is sufficiently violent to remove all correlation between momenta before and after the event. This model is applied only to gases, but another due to Gordon[2], based on the same principle, has been applied to liquids, and in some cases predicts Lorentzian or near-Lorentzian lineshapes. In such "impact" models, a Lorentzian lineshape, or, what is the same thing, an exponential time correlation function, may arise from the assumption that free rotations have a "lifetime", and that the number of rotors whose motions remain, at time t, uninterrupted since time 0, decays exponentially in t. The diffusion model which we have discussed, on the other hand, was seen to

predict an exponential correlation function through the solution of a differential equation (2.13) that describes aggregate motion over a large number of elementary rotations, and that does not take explicit account of the relative time durations of the individual rotational steps. Superficially, at least, it appears coincidental that both impact and diffusion models should lead to Lorentzian lineshapes: the linewidths obtained from the two models will differ starkly in physical significance. In any case, the fact that Lorentzian lineshapes may characterise the diametrically opposite processes of occasionally-interrupted free rotation in gases, and of small-step diffusive reorientation in liquids, urgently demonstrates that some criterion apart from mere lineshape must be called upon, to resolve whether rotational diffusion is a valid description of the motion. Two possible criteria are applied below.

I. <u>The Hydrodynamic Model:</u>

The hydrodynamic model simply relates rotational diffusion constants to the bulk viscosity of the fluid in question, by providing an estimate of the microscopic friction constants which may be used in (2.26). It is assumed that a molecule in solution may be treated in accordance with macroscopic hydrodynamics - i.e., that the shearing forces resisting its rotation may be calculated in the same way as they would be for a macroscopic body immersed in a fluid.

For a macroscopic sphere of radius a, immersed in a continuous, homogeneous, and stationary medium, Stokes calculated

$$\xi = 8\pi a^3 , \qquad \ldots (6.1)$$

where ξ is the drag constant (as discussed under V. of Ch. 2 - the drag tensor reduces to a scalar for a spherical body), and where η is the viscosity of the surrounding medium. Together with the relation (2.26) between diffusion and friction constants, this affords the "Stokes - Einstein" relation for the hydrodynamic diffusion constant:

$$D_h = kT / 8\pi\eta a^3 \qquad \ldots (6.2)$$

Agreement between (6.2) and the empirical diffusion constants, is usually construed as evidence supporting the rotational diffusion model,[3,4,5] since the hydrodynamic model explicitly assumes small-angle Brownian rotational diffusion in the calculation of ξ .

Hydrodynamic theory is applicable to large particles in a medium of small molecules. There is no rigorous proof that it applies also to small molecules in a solvent of molecules of approximately the same size. While the Stokes-Einstein calculation is generally acknowledged to be satisfactory for macromolecules in a solution of small, light molecules, its correctness is questionable elsewhere, since, for most liquids, the solute molecules are of roughly the same size as the solvent molecules, and also, since most molecules are nonspherical in shape. Aside from these relatively obvious objections, a doubtful view of the entire approach is taken by Steele[6] , who points out that the hydrodynamic result is obtained by assuming that there is no slip between the fluid and the surface of the body - thus, it is implicitly assumed that the angular dependence of the body-fluid interaction forces is sufficient to cause fluid molecules to follow the rotation of the body surface.

Some amelioration of these deficiencies is, however, possible:

(a) Perrin[7] generalised Stokes' law (6.1) for the sphere, to derive

the frictional drag tensor of an ellipsoid in terms of the medium viscosity and the particle dimensions, again on the basis of macroscopic hydrodynamics. Each frictional coefficient was found to be proportional to viscosity, so that, by (2.26), each of the principal diffusion constants depends inversely on viscosity (cf. (6.2)).

(b) Attention has been drawn[8] to the possibility of accommodating Steele's objection, noted above. While acknowledging that the usual "stick" or "no slip" boundary conditions, applied in the hydrodynamics calculation, may be inappropriate, the authors of Reference 8. consider there to be some evidence, that the Stokes-Einstein approximation holds more generally than would be expected from its derivation. Recent molecular dynamics calculations[9], for instance, indicate that if "slip" rather than the usual "stick" boundary conditions are used, the translational self-diffusion coefficient changes from $D=kT/6\pi a\eta$ to $D=kT/4\pi a\eta$, which is the correct result for hard-sphere fluids. The corresponding modification of the Stokes-Einstein result for rotational diffusion constants, however, does not appear yet to have been attempted in the literature.

(c) <u>Microviscosity Theory</u> - This fairly straightforward extension of the basic hydrodynamic theory has been applied with some success, in the synthesis of reorientational correlation times obtained from NMR[3] and Raman[4,5] experiments. Gierer and Wirtz[10] postulated a model for a spherical molecule of radius a, surrounded by concentric solvent shells of thickness 2b, obtaining

$$\xi = 8\pi\eta(T)\,a^3 f_r \ ,$$

where $f_r = \left[6\frac{b}{a} + \left(1+\frac{b}{a}\right)^{-3}\right]^{-1}$ is referred to as the "microviscosity correction"

to Stokes' law (6.1). For a neat liquid one has b=a, whence the "microviscosity" diffusion constant:

$$D_\mu = kT/\xi = 6.125\, kT/8\pi a^3 \eta(T) .$$

The factor $8\pi a^3$ is recognised as $6V_m$, where V_m is the volume of a single molecule. Usually V_m is calculated by assuming that Avogadro's number N of hexagonally close-packed spheres (filling 74% of space) occupy the molar volume M_w/ρ , where M_w is the molecular weight of the pure solute and ρ its density. Then, $V_m = .74 M_w/N\rho$.

$$\therefore D_\mu = 1.15 \times 10^8 \rho(T)\, T / M_w \eta(T) . \qquad \ldots (6.3)$$

The calculation of V_m on the basis of spherical molecules represents a serious assumption. Woessner et al.[11] have suggested that the result (6.3) for D_μ may be too large for nonspherical, elongated molecules, and recommend the application of a multiplicative correction factor less than unity. Without such correction, however, (6.3) has been found successfully to predict diffusion constants for reorientations that one would expect, in virtue of molecular geometry, to be highly hindered. Examples are the diffusion constants $D_\perp$ associated with tumbling motions (reorientations of the symmetry axis) of benzene[4], acetonitrile[5], and methyl iodide[12]. For these same molecules, on the other hand, it is found that (6.3) grossly underestimates the diffusion constants $D_\parallel$ associated with spinning motions (reorientations about the symmetry axis). This observation is in accord with the expectation that motions about a symmetry axis should be less hindered, and should therefore approach the "slip" boundary condition. A more probable interpretation however, is that such motions are not in the diffusion limit at all.

All the above variants of the basic hydrodynamic theory preserve the inverse dependence of D_h on viscosity as temperature changes. The modifying factor, however, is quite model sensitive; in practice, the adjustable parameters absorbed in it offer sufficient latitude to overlap any diffusion constant measurement taken at a single temperature. It has therefore been suggested[4] that a more meaningful test of the hydrodynamic theory, is whether it correctly predicts the temperature dependence of a diffusion constant. From this standpoint, the various hydrodynamic theories discussed above are all as one, in that all predict an inverse dependence of D_h on $\eta(T)$. The test usually reduces to a comparison of "activation energies", the significance of which is explained below.

Activation Energy:

The usual manner in which the temperature dependence of a diffusion constant is characterised, is by fitting it to an Arrhenius relation:

$$D(T) = D_o \exp(-E_a/kT) \quad , \qquad \ldots (6.4)$$

where E_a is the so-called "activation energy", and k is Boltzmann's constant. This relationship[13] is unabashedly phenomenological, and in fact is more compatible with a diffusion model we have not entertained - viz., the "activated jump" model - than with the Brownian motion model we have considered. (The activated jump model is generally believed[1] to be more applicable to rotation in solids than in liquids, except strongly hydrogen bonded liquids like water.) The motivation for the Arrhenius relation, in the jump model context, is at least transparent. If it is assumed that diffusion occurs in jumps over a potential barrier E_a , then the frequency of such jumps is proportional to the probability that a molecule will have sufficient rotational energy to surmount the

barrier. Hence the Boltzmann factor exp $(-E_a/kT)$.

Aside from the probability that the jump diffusion picture is organically wrong in the case of present interest, the Arrhenius relation is suspect on the grounds that the value of E_a might itself be temperature-dependent, especially in an experiment like the present one, in which temperature does not vary alone, but also induces a concomitant variation in density. (If the average size of interstices between molecules changes, the intermolecular potential changes, and probably also E_a.) Nonetheless, if E_a varies but slowly with T, the empirical diffusion constant may conform reasonably well to (6.4) over a limited temperature range. In practice, this is what is generally found. Thus, while one should be chary of interpreting the empirical value of E_a, found in a fit to (6.4), as an activation energy in the precise sense indicated above, this value is still a useful parameter for the concise description of D(T) in a specific temperature range.

We evaluate the applicability of the hydrodynamic model to tumbling motions of benzene, by fitting the diffusion constants $D_\perp$ we have derived from linewidth analysis, to the Arrhenius relation, and comparing the resultant value of E_a with the value obtained by fitting the microviscosity diffusion constant D_μ to the same relation over a similar temperature range. The value of D_μ has been computed from (6.3), with available literature values of benzene density $\rho(T)$ [14] and of benzene-carbon tetrachloride mixture viscosity $\eta(T)$ [15]. The fits have been performed by applying linear regression to the logarithm of (6.4):

$$\ln D = \ln D_0 - \left(\frac{E_a}{k}\right) T^{-1}.$$

The value of E_a is a measure purely of the temperature dependence of D, as it would be unaffected by a change in the proportionality constant D_o. The activation energies for the various mixture proportions are displayed below, the empirical values (from $D_\perp(T)$) in Table 3, and the hydrodynamic values (from $D_\mu(T)$) in Table 4. These results are also plotted in Fig. 6. The errors indicated, are the greater of the internal and external errors for the empirical results, and the external errors for the hydrodynamic results (since the literature sources did not state the errors of the $\rho(T)$ and $\eta(T)$ data).

TABLE 3

Empirical Activation Energies

Mole fraction C_6H_6	1.00	.81	.62	.42	.21
E_a(kcal./mole)	2.3±1.3	1.4±.6	.7±.8	0.0±.5	.7±.5

TABLE 4

Hydrodynamic Activation Energies

Mole fraction C_6H_6	1.00	.81	.61	.36	0.00
E_a(kcal./mole)	2.86±.03	2.91±.03	2.97±.01	2.93±.02	2.86±.02

For pure benzene, the hydrodynamic estimate of E_a agrees with the experimental determination, within experimental error. But while the hydrodynamic estimate remains virtually constant with progressive dilution, the experimental value decreases strongly. Thus, our results are consistent with a diffusive rotational Brownian motion model for pure benzene, but it would appear that another mechanism is operative in benzene-carbon tetrachloride mixtures. Further consideration will be given in III. to the results for mixtures.

FIG. 6

Concentration dependence of the hydrodynamic and the empirical activation energies.

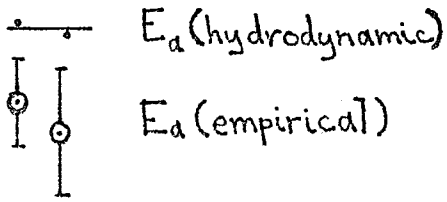

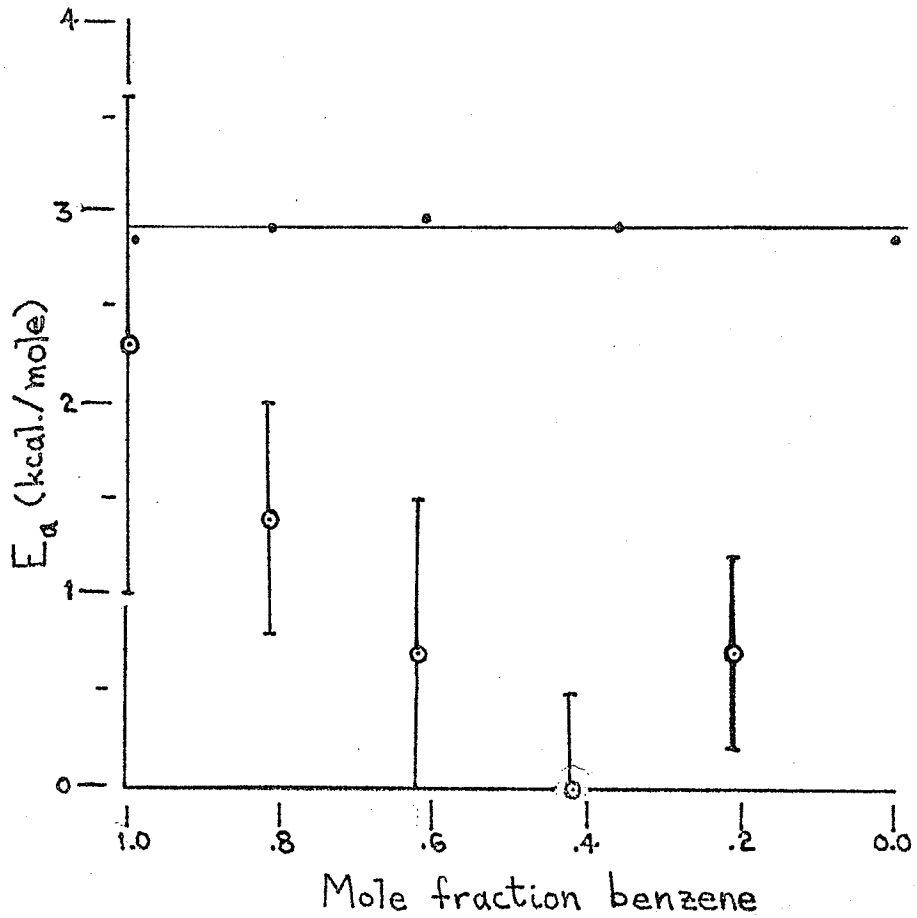

Although, as indicated earlier, not too much significance should be attached to the numerical agreement of $D_\perp$ and D_μ at a single temperature, it is nonetheless interesting to compare these values for pure benzene. The experimental values appear (Fig. 7) to be in reasonable proximity of the microviscosity values.

II. The χ - test:

A second criterion against which to judge the applicability of the rotational diffusion model, is the χ-test[3]. This consists in a comparison of the empirical reorientational correlation time $\tau_{or}=1/6D_i$ for motion about the i'th axis, to the theoretical reorientation time $\tau_f = \frac{41}{360}\times 2\pi(I_i/kT)^{\frac{1}{2}}$ for a free rotor, at the same temperature. (Both these times are defined as the time for a symmetric-top orientational correlation function $\langle Tr[\vec{\beta}(0)\cdot\vec{\beta}(t)]\rangle$ to fall off by the factor e^{-1}. Since this occurs[16] when the symmetry axis has reoriented through a net angular displacement of 41°, τ_f is just the time taken by an "average" free rotor, for which $\frac{1}{2}I_i\omega_i^2 = kT/2$, to rotate through 41°.).

One defines the parameter χ_i by

$$\chi_i = \frac{\tau_{or}}{\tau_f} = \frac{30}{41\pi D_i}\left(\frac{kT}{I_i}\right)^{\frac{1}{2}}. \qquad \ldots (6.5)$$

It is clear that a value of χ_i much larger than unity is expected if reorientation about the i'th axis is diffusive: for; if the direction of rotation changes randomly in the course of a small angular displacement, then the total angular displacement $\int|\vec{\omega}|dt$ executed during a net reorientation of 41°, will be much larger than 41°, and will correspondingly occupy a much longer time than a free rotation through 41°.

The significance of χ_i can, moreover, be made quantitative: in the diffusion limit, it bears a simple relation to the size of an individual

FIG. 7

Temperature dependence of the microviscosity (D_μ) and the empirical ($D_\perp$) diffusion constants, for pure benzene.

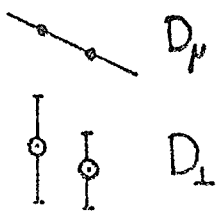

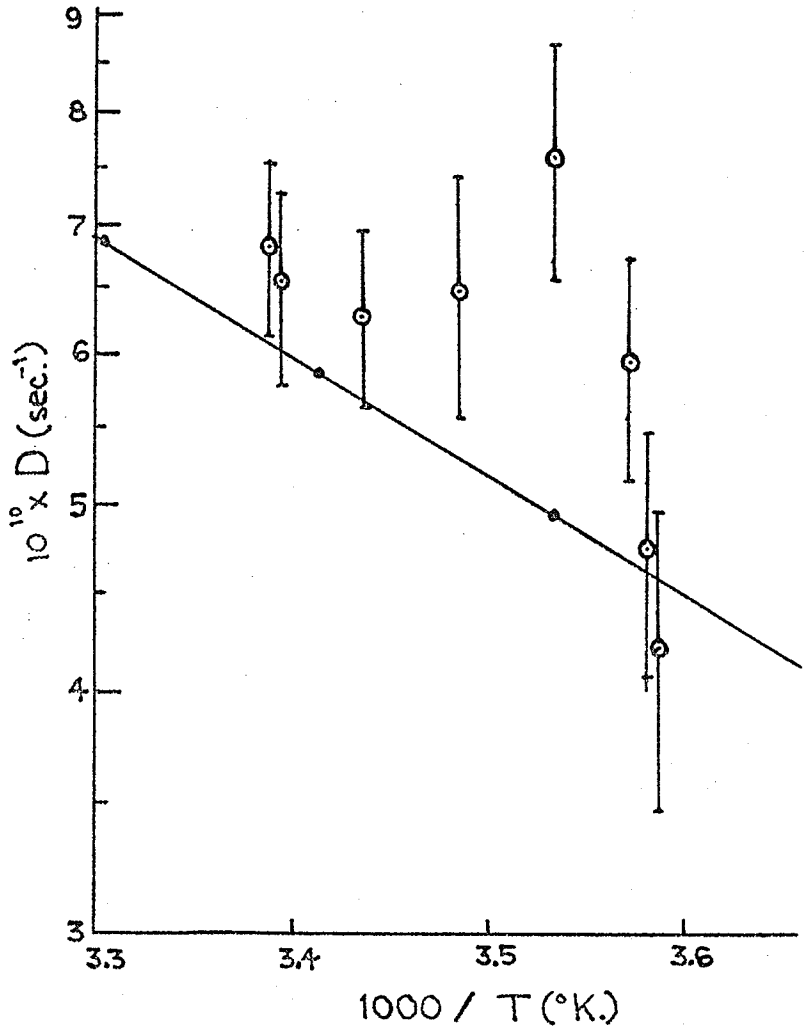

angular step. To see this, one supposes that the direction of angular momentum is randomised at the end of each step. It follows readily that the angular momentum correlation time is just the mean time duration of a single angular step. From (2.25), then, the mean duration of an angular step about the i'th axis is

$$\tau_i = I_i / \xi_i \ .$$

To realise an estimate of the mean angular step size, we multiply this duration by an expectation value $\bar{\omega}_i$ for the i'th angular velocity component. We assume that, during a diffusive step, ω_i is distributed as it would be for an ensemble of free rotors. Under such conditions, it was found in V. of Ch. 2 that

$$\langle \omega_i^2 \rangle = kT / I_i \ .$$

Accordingly, we use for $\bar{\omega}_i$ the r.m.s. value of ω_i; our estimate of the mean angular step size is

$$\langle \Delta\theta_i \rangle = \tau_i \bar{\omega}_i = \frac{I_i}{\xi_i}\left(\frac{kT}{I_i}\right)^{\frac{1}{2}} = \left(\frac{kT}{\xi_i}\right)\left(\frac{I_i}{kT}\right)^{\frac{1}{2}} \ .$$

Recalling (2.26), we obtain (in radians)

$$\langle \Delta\theta_i \rangle = D_i \left(\frac{I_i}{kT}\right)^{\frac{1}{2}} \ .$$

Comparison with (6.5) reveals that

$$\langle \Delta\theta_i \rangle = \left(\frac{41\pi}{30}\chi_i\right)^{-1} = \frac{1}{4.29\,\chi_i} \ . \qquad \ldots (6.6)$$

With a view to interpretation of the value of χ_i in terms of the nature of the reorientation process, the following, more or less arbitrary, guidelines have been suggested[3]:

$\chi < 2.5 \rightarrow$ "inertial" (free rotor) behaviour;

$2.5 < \chi < 4.2 \rightarrow$ "intermediate" region;

$4.2 < \chi \rightarrow$ diffusive reorientation.

Using the values of $D_\perp$ displayed in Table 2, and a literature value[17] for the inertial moment of a benzene molecule about an axis perpendicular to the symmetry axis, we have found, for pure benzene, that the value of χ ranges from about 5.6 at 295°K. to 8.8 at 279°K. These results strongly support the view that tumbling reorientations in pure benzene are diffusive in nature. By (6.6), the mean angular step sizes range from about .042 radians (=2.4°) at 295°K., to about .026 radians (=1.5°) at 279°K.

Interpretation of the results of the χ-test for C_6H_6-CCl_4 mixtures, however, poses a quandary. It will be recalled from I. that the hydrodynamic model did not compare favourably with the experimental results for mixtures; thus, the diffusion hypothesis was not supported by this comparison. But it is apparent that the empirical value of $D_\perp$, and hence of χ, at room temperature, does not change significantly with benzene concentration. According to the present criterion, then, if rotational diffusion provides a valid description of reorientation in pure benzene at room temperature, so must it for mixtures at room temperature. The tendency of χ to rise as temperature falls, however, is markedly less pronounced in the mixtures than in pure benzene; the temperature trend is in fact essentially flat for the most dilute (21% benzene) mixture studied. Thus, diffusive reorientation is not so strongly indicated in the mixtures as in pure benzene, at lower

temperatures.

It may well be the case that the angular step size cannot be inferred so reliably from (6.6) for mixtures, as for pure benzene. The shape of a CCl_4 molecule is more nearly spherical than that of a C_6H_6 molecule; therefore, the interaction forces between a C_6H_6 and a neighbouring CCl_4 molecule, due to steric hindrance by one molecule of the reorientations of the other, will be less impulsive in nature than the forces between two C_6H_6 molecules. For this reason, the picture of discrete angular steps terminated instantaneously by an interaction that randomises the angular momentum of the rotor, to which we appealed in the derivation of (6.6), may be a poor model of the situation for mixtures. Accordingly, we deem it a moot point, whether the results of the χ-test indicate diffusive reorientation in the mixtures.

Finally, we investigate an alternative model to rotational diffusion, to rationalise the temperature dependence of $D_\perp$ in the mixtures.

III. Dynamically Coherent Reorientation - The SDFR Model:

A theory has been advanced by Steele[18] to treat motion in the opposite theoretical limit to rotational diffusion - viz., the "slightly damped free rotation" (SDFR) model. This model postulates "dynamically coherent" reorientation, in which the angular velocity component under consideration remains constant over a long period of time. It has been applied successfully to the spinning motions (reorientations about the symmetry axis) of benzene[4], acetonitrile[5], and methyl iodide[12], for which, as mentioned in I., the diffusion model was found to fail. The motivation for applying the SDFR model to tumbling motions of benzene in C_6H_6-CCl_4 mixtures, is just the reason cited in II. above, for which the results of the χ-test on mixtures are suspect: one no longer expects

angular steps to be terminated by sharp, instantaneous changes in angular velocity.

The result of the SDFR theory, germane to our present considerations, is the reorientational correlation time

$$\tau_{or} = \frac{41}{360} \times 2\pi \left(\frac{I_i}{kT}\right)^{\frac{1}{2}} ,$$

which is merely the time taken by a free rotor with angular velocity $\sqrt{\langle \omega_i^2 \rangle} = (kT/I_i)^{\frac{1}{2}}$ to execute a rotation through the correlation angle 41° about the i'th axis. The corresponding diffusion constant, by (2.21), is

$$D = \frac{1}{6\tau_{or}} = \frac{30}{41\pi}\left(\frac{kT}{I_i}\right)^{\frac{1}{2}} . \qquad \ldots (6.7)$$

It should be noted at the outset that the diffusion constant predicted by (6.7) is about five times too large to match our empirical results for tumbling motions of benzene. Dismissal of the SDFR hypothesis on this basis, however, may be premature. It is interesting to evaluate the SDFR model, as we did the hydrodynamic model, in respect of the temperature dependence it predicts for $D_\perp$. As in I., we shall compare the activation energy value predicted by our model, with the empirical results shown in Table 3.

To derive the SDFR activation energy, one takes the logarithm of (6.4):

$$\ln D = \ln D_o - \frac{E_a}{k} T^{-1} ,$$

so that $$-\frac{E_a}{k} = \frac{d}{d(T^{-1})} (\ln D) .$$

From (6.7) one has

$$\ln D = \ln\left(\frac{30\, k^{\frac{1}{2}}}{41\pi I_i}\right) + \frac{1}{2} \ln T .$$

Hence, $$E_a = -\frac{k}{2}\frac{d}{d(T^{-1})}(\ln T)$$

$$= \frac{kT}{2} \qquad \text{for a single rotor,}$$

or $$E_a = \frac{RT}{2} = .29 \text{ kcal. per mole of rotors,}$$

at room temperature. This value is consistent with the experimental results (Table 3) for the three lowest benzene concentrations. By this reckoning, it appears reasonable to interpret the observed trend of E_a with decreasing benzene concentration, as an approach to the free rotor limit.

References:

1. W. A. Steele in "Transport Phenomena in Fluids", edited by H. J. M. Hanley (Marcel Dekker, New York and London, 1969).
2. R. G. Gordon, J. Chem. Phys. 44, 1830 (1966).
3. K. T. Gillen and J. H. Noggle, J. Chem. Phys. 53, 801 (1970).
4. K. T. Gillen and J. E. Griffiths, Chem. Phys. Letters 17, 359 (1972).
5. J. E. Griffiths, J. Chem. Phys. 59, 751 (1973).
6. W. A. Steele, J. Chem. Phys. 38, 2404 (1963).
7. F. Perrin, J. Phys. Radium 5, 33 (1934).
8. G. R. Alms, D. R. Bauer, J. I. Brauman, and R. Pecora, J. Chem. Phys. 58, 5570 (1973).
9. B. J. Alder, D. M. Gass, and T. E. Wainwright, J. Chem. Phys. 53, 3813 (1970).
10. A.Gierer and K. Wirtz, Z. Naturforsch. A8, 532 (1953).
11. D. E. Woessner, B. S. Snowden, Jr., and E. T. Strom, Mod. Phys. 14, 265 (1968).
12. J. E. Griffiths, Chem. Phys. Letters 21, 354 (1973).
13. P. A. Egelstaff, "An Introduction to the Liquid State" (Academic Press, London and New York, 1967), p. 151.

14. Handbook of Chemistry and Physics, 44th Ed. (Chemical Rubber Publ. Co., Cleveland, Ohio, 1962), p. 2334.

15. Thorpe and Rodger, Trans. Chem. Soc. 71, 360 (1897).

16. F. J. Bartoli and T. A. Litovitz, J. Chem. Phys. 56, 413 (1972).

17. G. Herzberg, "Electronic Spectra and Electronic Structure of Polyatomic Molecules" (D. Van Nostrand Co., Inc., Princeton, New Jersey, 1967), p. 666.

18. W. A. Steele, J. Chem. Phys. 38, 2411 (1963).

CHAPTER 7

DISCUSSION - VIBRATIONAL RELAXATION

In this chapter, our concern is with the information recumbent in the isotropic scattering, available to us (cf.(2.5b)) through the polarised spectrum. The structure of the isotropic spectrum, as shown by (2.10a), is governed by the time correlation of the appropriate vibrational coördinate. Broadening of the isotropic spectrum, then, is due to the loss of such correlation, which occurs as a result of vibrational relaxation. Accordingly, we may obtain from the isotropic lineshape, information about the time scale on which such relaxation processes take place. Contemporary understanding of vibrational relaxation mechanisms is not greatly advanced[1]; consequently, the present treatment will be largely qualitative.

Isotropic lineshapes were found to conform well to a Lorentzian, when fitting was performed on the structure-free side, and when instrumental correction was essayed in the manner outlined in I.A. of Ch. 4. The isotropic linewidth (FWHM) results Γ_{iso} are recorded in Table 1, for the various temperatures and benzene concentrations at which the experiment was performed. Also, the results are presented graphically in Fig. 8, where linear fits have been superimposed to illustrate the temperature variation of Γ_{iso} at each concentration. Over the limited temperature range studied, the data were generally found to be supportive only of, and adequately described by, a linear fit. One notable exception was encountered: the 21% benzene linewidth suffers an abrupt reduction as temperature falls below about 270°K. This is possibly due to a change in the nature of the solution resulting from the onset of dimerisation; it should be pointed out, however, that our experiments

FIG. 8

Temperature dependence of the isotropic linewidth, at various concentrations.

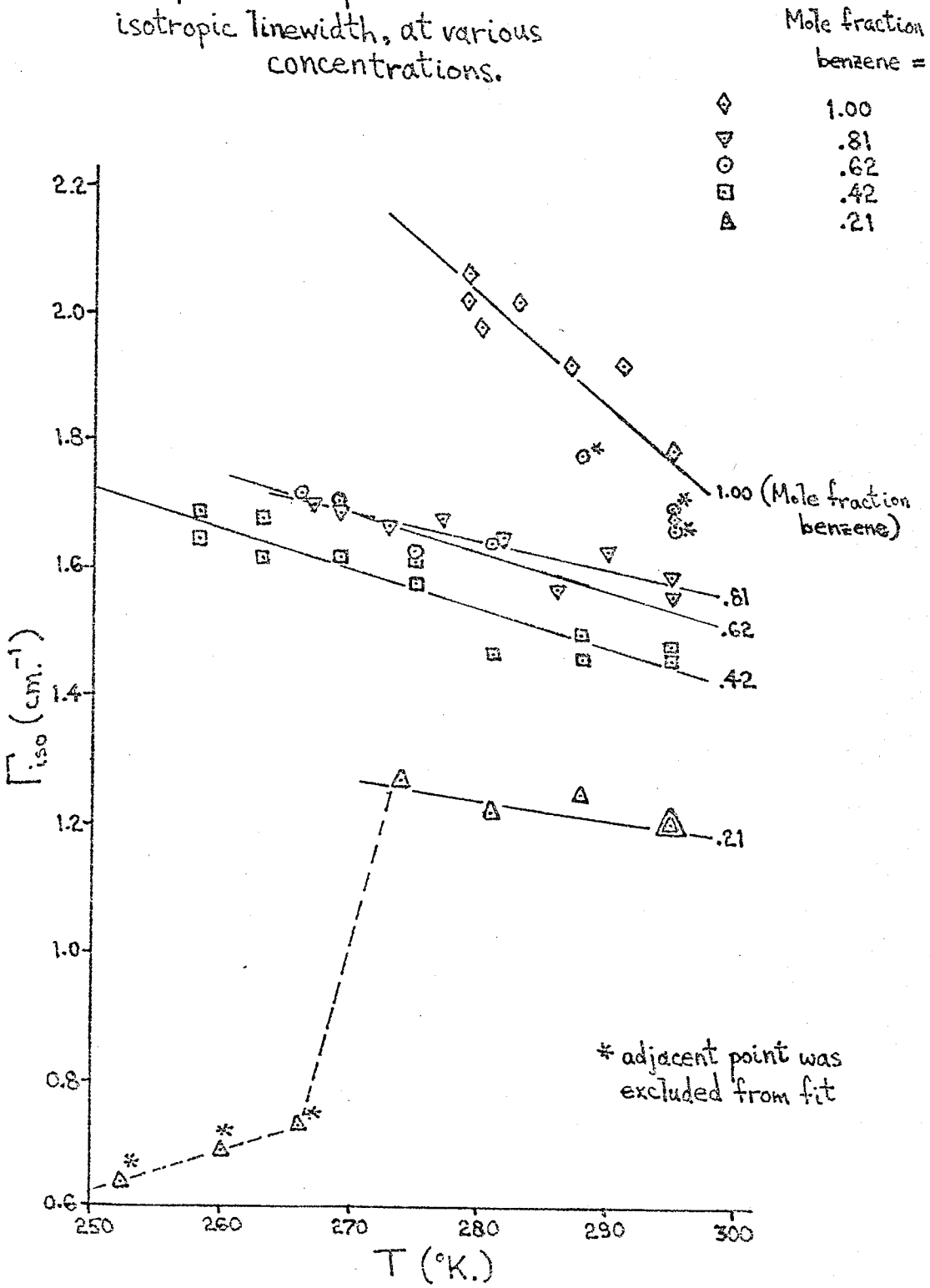

were apparently confined to a temperature range within which dimerisation was not expected to occur (cf. B.5. of Ch. 3), and that the accuracy of our temperature measurements was confirmed by observations of the freezing points of the various solutions. Finally, the concentration dependence of Γ_{iso}, at 295°K., is plotted in Fig. 9, and a regression line superimposed to illustrate the trend.

The gross patterns evident in the linewidth results are as follows:

(i) At a given concentration, Γ_{iso} decreases with increasing temperature.

(ii) At a given temperature, Γ_{iso} decreases as concentration decreases.

(iii) The slope $d\Gamma_{iso}/dT$ decreases sharply upon initial dilution with CCl_4, but remains roughly constant thereafter (Table 5):

TABLE 5

Slope of Γ_{iso} vs. temperature

Mole fraction C_6H_6	1.00	.81	.62	.42	.21
$10^3 X d\Gamma_{iso}/dT$ (cm.$^{-1}$/°K.)	-17.±4.	-4.5±.8	-5.9±2.1	-6.1±.9	-2.8±2.2

Trend (i) has been noted previously in the case of pure CH_3I by Wright et al.[2], and by Campbell et al.[3] Trend (ii) has been observed by Griffiths et al.[4] for C_6H_6 in solution with C_6D_6.

The implications of these trends will be explored in following sections (III. and IV.). Preliminary to this, however, we undertake a critical examination (in I.) of our linewidth measurements, and discuss (in II.) the vibrational relaxation mechanisms, in terms of which the observed linewidth trends may be rationalised.

I. <u>The Linewidth Measurement:</u>

Since numerous measurements of the isotropic linewidth of the 992 cm.$^{-1}$

FIG. 9

Concentration dependence of the isotropic linewidth, at room temperature.

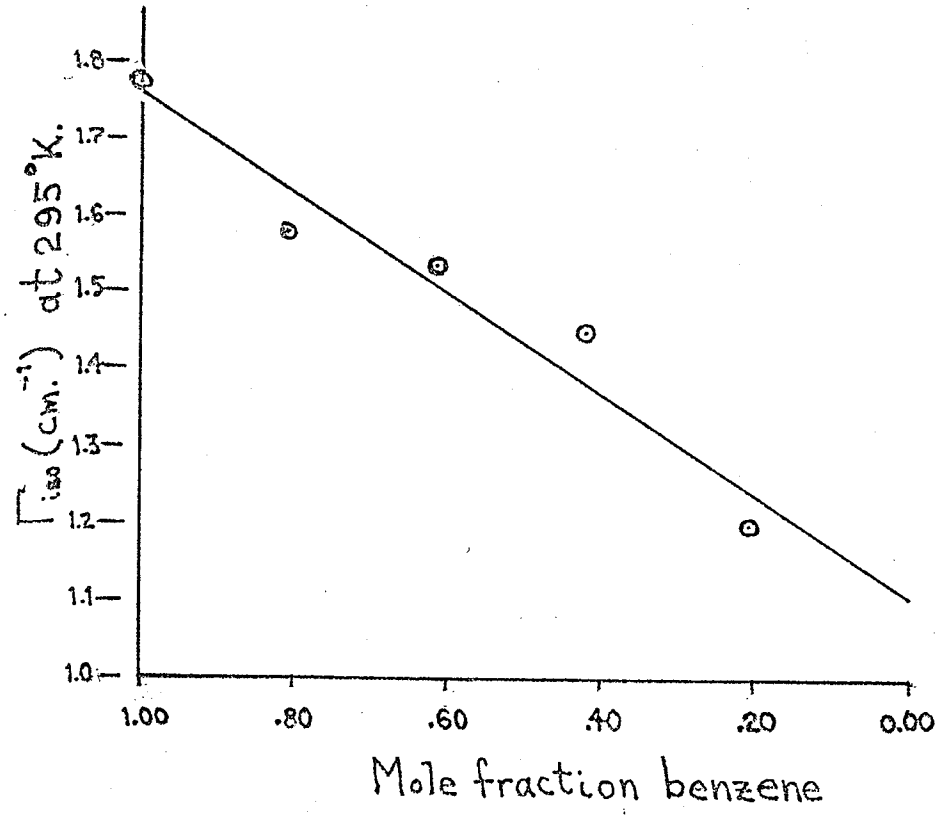

benzene line appear in the literature, it is in order to compare our results, in instances where this is possible, with available literature values. We have done so, for pure benzene at RTP. One encounters a disconcerting degree of variation among reported values of this width. The earlier measurements[5] were performed with mercury arc excitation sources, and yielded widths around 1.8 $cm.^{-1}$ It should be noted that the breadth of the excitation line, relative to the benzene line in question, would render unavoidable the use of a deconvolution technique, accurately to recover the true benzene lineshape, if such a source were used. Frenzel et al.[6], using laser excitation and carefully adjusted monochromator slits, found $\Gamma_{iso} = 1.5$ $cm.^{-1}$ Clements and Stoicheff[7] have made a high resolution interferometric measurement with laser excitation, and have found $\Gamma_{iso} = 2.15 \pm .15$ $cm.^{-1}$ Griffiths , using the "zero slit-width extrapolation" (ZSE) method (cf. I.A.1. of Ch. 4), has obtained $\Gamma_{iso} = 2.24 \pm .1$ $cm.^{-1}$ The weighted average of our room temperature results for pure benzene is $\Gamma_{iso} = 1.74 \pm .03$ $cm.^{-1}$; if we average through the assumed linear dependence on temperature, using the regression result at 295°K., we get $\Gamma_{iso} = 1.77 \pm .06$ $cm.^{-1}$

Despite first appearances, we consider our determination to be consistent with the laser excitation results of References 4. and 7., when careful account is taken of what is actually measured in the several experiments. The ZSE method of Griffiths, as pointed out in I.A.1. of Ch. 4, may be expected to overestimate Γ_{iso} by the laser linewidth plus the diffraction limit of the monochromator. Under the usual conditions of contemporary laser Raman experiments, the width of the argon ion laser line is about 0.15 $cm.^{-1}$, and the diffraction limit of the double monochromator is about 0.25 $cm.^{-1}$ Therefore, the ZSE

estimate is approximately 0.4 $cm.^{-1}$ too high. Griffiths has, however, removed the broadening contribution of the 993 $cm.^{-1}$ hot band on the high-frequency-shift side, by fitting only on the structure-free (low-shift) side. We have adopted the same strategy in respect of the hot band, and therefore expect our measurement, from which laser line and slit broadening have been removed by deconvolution, to differ from Griffiths' only by the 0.4 $cm.^{-1}$ inherent in the ZSE estimate. Our result is in good agreement with this expectation. Clements and Stoicheff, on the other hand, apparently do not remove the 993 $cm.^{-1}$ hot band; our results were similar to the Stoicheff value when fitting was performed over the entire profile, rather than on the structure-free side, so that the hot band would seem to account for the discrepancy in this case. The reason for the extremely low value obtained by Frenzel et al. remains unclear.

II. Vibrational Broadening Mechanisms:

Many models have been proposed for vibrational energy transfer among polyatomic molecules.[8] One mechanism often considered dominant in gases and liquids involves a vibration-translation (V-T) transfer process.[9] A rapid intramolecular transfer of vibrational energy is thought to maintain an equilibrium energy distribution among the fundamental vibrational modes of an excited molecule. During a collision with another molecule, the total vibrational energy undergoes a vibration-to-translation relaxation process through the lowest energy vibrational mode. The process has been widely studied, especially through ultrasonic methods.[8] Litovitz[10] has developed a binary collision model, which has provided a basis for elucidation of this process.

Griffiths[4] has recently suggested that another mechanism may also be operative in the liquid phase. At high densities, where the time

between collisions becomes short, intermolecular vibration-to-vibration (V-V) energy transfer may dominate the energy cascade. During a collision between two molecules, vibrational energy will be more readily transferred from an excited energy level of one molecule to a lower level of the other, if the two levels involved are close together, than if they were widely spaced. The energy difference would be transferred to translational energy if this interaction were successful.

Griffiths has provided an illustration of the latter mechanism in mixtures of C_6H_6 and C_6D_6. The linewidths of the ν_2 fundamentals for pure C_6H_6 and pure C_6D_6, at room temperature, were measured to be 2.24 $cm.^{-1}$ and 1.52 $cm.^{-1}$ respectively; the difference is larger than would be expected for two such similar molecules, if only the V-T relaxation mechanism prevailed. In C_6H_6, there are two vibrational energy levels, ν_7 (985 $cm.^{-1}$) and ν_{19} (970 $cm.^{-1}$), slightly below the ν_2 (992 $cm.^{-1}$) level. These nearby levels might give play to the V-V mechanism. By contrast, in C_6D_6, the closest level to the ν_2 (945 $cm.^{-1}$) level is the higher ν_6 (963 $cm.^{-1}$) level; no other C_6D_6 levels lie in the immediate vicinity, either of the ν_2 level of C_6D_6, or of the ν_2 level of C_6H_6. For this reason, it is expected that the V-V relaxation mechanism will be important only in C_6H_6-C_6H_6 collisions, not in C_6H_6-C_6D_6 or C_6D_6-C_6D_6 collisions. Griffiths proposes that the V-V process, operating preferentially in C_6H_6-C_6H_6 collisions, accounts for the difference between the linewidths of pure C_6H_6 and pure C_6D_6. To support this point of view, he has measured the isotropic ν_2 linewidths of both species in C_6H_6-C_6D_6 mixtures, as a function of relative concentration. The observed result is that the C_6H_6 linewidth depends linearly on the mole fraction of C_6H_6, while the C_6D_6 linewidth remains constant. Extrapolated to 0% C_6H_6, the

C_6H_6 linewidth equals that of C_6D_6. A tidy synthesis of these results is provided by Griffiths' proposal. At high C_6H_6 concentrations, where numerous C_6H_6-C_6H_6 collisions occur, both the V-V and V-T mechanisms contribute to vibrational relaxation in C_6H_6. Upon dilution, the number of such collisions undergone by a given C_6H_6 molecule diminishes, and hence also the contribution of the V-V mechanism to C_6H_6 relaxation. Such collisions are, however, largely replaced by C_6H_6-C_6D_6 collisions. The structural similarity of C_6H_6 and C_6D_6 impels the expectation, that the probability for a C_6H_6 molecule to undergo V-T relaxation during a collision, is independent of whether the other collision partner is a C_6H_6 or a C_6D_6 molecule. Thus, the V-T broadening contribution to the C_6H_6 linewidth should be independent of concentration. The net effect of dilution is that, overall, collisions become less efficient in inducing C_6H_6 relaxation, since one mechanism declines in importance, while the other remains the same. Associated with this reduction in relaxation efficiency is an increase in vibrational lifetime, and hence a decrease in C_6H_6 linewidth. At infinite dilution (0% C_6H_6), the V-T mechanism operates exclusively, and the situation, for C_6H_6 relaxation, is identical to that which governs C_6D_6 relaxation throughout the concentration range. Hence, the two linewidths should intersect at infinite dilution; this is in accord and Griffiths' observations.

III. Concentration Dependence Of Benzene ν_2 Relaxation Rate In C_6H_6-CCl_4 Mixtures:

The present linewidth data for the ν_2 line of benzene in C_6H_6-CCl_4 mixtures, afford a further opportunity to examine Griffiths' hypothesis. In Fig. 9, Γ_{iso} appears as a function of C_6H_6 concentration, at 295°K. (The individual point plotted for each concentration was read off the

temperature trend line (Fig. 8) for that concentration, and not taken directly from Table 1.) As with the C_6H_6-C_6D_6 system examined by Griffiths, a linear trend emerges. The equation of this regression line is

$$\Gamma_{iso} = (1.11 \pm .04) + (.647 \pm .067)f \quad ,$$

where f is the mole fraction of C_6H_6.

Similarly, performing linear regression on Griffiths' data for the C_6H_6 linewidth in C_6H_6- C_6D_6 mixtures, we obtain

$$\Gamma_{iso} = 1.52 + .742\ f.$$

A comparison of these two trend lines is interesting on several counts. First, the two slopes match within experimental error. Thus, the rapidity of vibrational relaxation depends similarly, in the two cases, on the frequency of C_6H_6- C_6H_6 collisions. Second, over the entire range of f, the difference between our (regression) value for Γ_{iso} and that of Griffiths is roughly constant, at about 0.4 $cm.^{-1}$ This observation confirms our comments in II. regarding the overestimation of linewidth inherent in the ZSE method. Third, both C_6H_6-C_6D_6 and C_6H_6-CCl_4 collisions apparently yield similar relaxation rates. De-excitation of the ν_2 level of C_6H_6 is, therefore, presumably insensitive to the details of the interaction with these two different partners. This is consistent with the usual view that, since the most auspicious condition for a successful V-T interaction is a particularly violent collision, enough distortion of the colliding molecules is apt to occur that their equilibrium structural details are, so to speak, forgotten during the interaction.

IV. Temperature Dependence of the Relaxation Rate:

From Table 5, it is apparent that the slope $d\Gamma_{iso}/dT$ is negative for all concentrations of C_6H_6. For pure C_6H_6, its magnitude is largest; it decreases sharply upon initial dilution, but changes only moderately thereafter.

To interpret this behaviour in relation to possible relaxation mechanisms, we have followed a treatment of pure CH_3I given by Campbell, Fisher, and Jonas[3]. These authors have found in the case of CH_3I that the relaxation rate $1/\tau_{vib}$ ($\sim \Gamma_{iso}$) decreases as temperature increases. In analysing their results, they invoke the binary collision model of Litovitz[10] for the V-T process. According to this model, the relaxation rate may be expressed as

$$\frac{1}{\tau_{vib}} = P_{1-0}(T)N\left[1-\exp(h\nu/kT)\right],$$

where N is the collision frequency and P_{1-0} is the probability per "hard" collision that a molecule in the first excited vibrational state having frequency ν will go to the ground state upon collision. The probability P_{1-0} is assumed to be a function of temperature but not of density. It has been shown[11] that the harsher or more sudden the interaction, the higher is the probability that a transition will occur: P_{1-0} is a strong function of temperature, and dP_{1-0}/dT is positive.

To account for their observation that the relaxation rate falls as T rises, despite the rise of P_{1-0} with T (and the concomitant increase in $[1-\exp(h\nu/kT)]$), Campbell et al. demonstrate that the collision frequency N may decrease with increasing temperature, because of a decrease in the molecular hard sphere diameter σ. Together with the decrease in density associated with a rise in temperature, a decrease in σ would imply a longer free path between collisions, and might

therefore result in a longer time between collisions and a lower relaxation rate, if the countervailing increase in mean translational velocity did not predominate. That σ should decrease as temperature rises, is expected in virtue of the finite slope the intermolecular potential: because of this slope, the increase in mean translational kinetic energy that accompanies a rise in temperature, allows molecules to approach one another more closely before reaching the classical turning point. In view of the close packing of molecules in a liquid, a small change in σ may represent a significant increment in the mean free path between collisions. Campbell et al. have calculated the collision frequency N, as predicted by several models of liquid dynamics (the cell model, the Enskog model, and the J-diffusion model), and have estimated P_{1-0} from gas phase studies[8]. They conclude that, as temperature increases at constant pressure, the increase in time between collisions, due to the changes in density and hard sphere diameter, prevails against the competing rise in P_{1-0} .

We have treated our pure C_6H_6 data in a similar fashion, but have been unable to elicit even qualitative agreement with the binary collision model for the V-T process. In order simultaneously to accommodate the value of Γ_{iso} at 295°K., and the slope $d\Gamma_{iso}/dT$, negative values of dP_{1-0}/dT must be postulated, whether the cell model or the Enskog model is used in the calculation of N. This negative result reinforces the suggestion made earlier, that an unusual relaxation mechanism, such as the V-V process discussed in II. and III. above, is operative in C_6H_6-C_6H_6 encounters.

The mixture data is more difficult to analyse, even qualitatively. Upon dilution, the C_6H_6-C_6H_6 collisions become less frequent and the

relaxation rate approaches a value, presumably characteristic of the V-T mechanism. For pure C_6H_6, the large negative slope of $d\Gamma_{iso}/dT$ suggests that the temperature dependence of the relaxation rate is governed primarily by the behaviour of the collision frequency, and that the transition probability for a V-V interaction is not a strong function of temperature. As the V-T process becomes relatively more important with progressive dilution, dP_{1-0}/dT, which is positive, begins to offset dN/dT, which is negative, in determining the net slope $d\Gamma_{iso}/dT$: hence the observed reduction (Table 5) in magnitude of the slope, upon dilution.

References:

1. S. Ormonde, Rev. Mod. Phys. 47, 193 (1975).
2. R. B. Wright, M. Schwartz, and C. H. Wang, J. Chem. Phys. 58, 5125 (1973).
3. J. H. Campbell, J. F. Fisher, and J. Jonas, J. Chem. Phys. 61, 346 (1974).
4. J. E. Griffiths, M. Clerc, and P. M. Rentzepis, J. Chem. Phys. 60, 3824 (1974).
5. J. D. Masso, Y. D. Harker, and D. F. Edwards, J. Chem. Phys. 50, 5420 (1969).
6. C. A. Frenzel, E. B. Bradley, and M. S. Mathur, Appl. Spectry. 25, 614 (1971).
7. W. R. L. Clements and B. P. Stoicheff, Appl. Phys. Letters 12, 246 (1968).
8. T. L. Cottrell and J. C. McCoubrey, "Molecular Energy Transfer in Gases" (Butterworth and Co. Ltd., London, 1961).
9. K. Herzfeld and T. A. Litovitz, "Absorption and Dispersion of Ultrasonic Waves" (Academic Press, New York, 1959).
10. T. A. Litovitz, J. Chem. Phys. 26, 469 (1957).
11. P. K. Davis and I. Oppenheim, J. Chem. Phys. 57, 505 (1972).

CHAPTER 8

CONCLUSIONS

1. On the molecular dynamics of benzene, and of benzene-carbon tetrachloride mixtures:

   Our results confirm that tumbling motions of benzene in the neat liquid are in the rotational diffusion limit, but suggest that, upon dilution with carbon tetrachloride, such motions approach free rotor behaviour. The observed temperature and concentration dependence of the vibrational relaxation rate supports the view that an unusual relaxation mechanism, such as a vibration-to-vibration energy transfer, operates in C_6H_6-C_6H_6 interactions.

2. On possible refinement of the present experiment:

   The improvement which is most clearly required, is a reduction in the stray light component of the measured depolarised spectrum. The large stray light throughput that was experienced, occasioned most of the analysis problems encountered in the present work. We consider that our "Method (1)" analysis of depolarised spectra, could not have failed so abjectly in the absence of stray light. In any case, it is more desirable in principle, to remove stray light at the source, than to compensate for it analytically after the fact. We consider that scrupulous design of the sample cell would be helpful in the reduction of stray light. It should be recognised, however, that the 992 $cm.^{-1}$ line of benzene, because of its extreme polarisation, presents as severe a stray light problem as would ever be encountered. The analytical methods developed in the present work should therefore be satisfactory in any other case, if they perform acceptably in the present case.

An improvement in resolution of the polarised spectra could be effected, if they were studied at reduced slit-widths. Ample intensity is available to permit such a reduction. (Broad slits were used in the present work to enable the application of "Method (2)" analysis to the depolarised spectra; the polarised spectra were of secondary interest.)

Finally, it would be helpful to extend the temperature range of the experiment by heating samples above room temperature.

3. Proposals for further work:

It would be interesting to study reorientational broadening of the Rayleigh line, in order to investigate the importance of angular coöperative effects. Agreement with the Raman results would indicate that such effects were insignificant. Moreover, the Rayleigh line might provide a convenient means to study reorientation in dilute solutions, since the reduction in intensity with dilution would not present the problem it does in the study of the much weaker Raman lines, and since dilution with a solvent of spherical molecules might eliminate angular coöperative effects.

Comparison of Raman with infrared orientational broadening can provide a test of whether reorientational motion is diffusive in nature.[1]

Raman studies of additional vibrational modes, possibly applying the Rakov technique[2] to depolarised lines, may be used to determine the complete diffusion tensor of benzene.

Examination of the reorientational behaviour of CCl_4, as well as C_6H_6, in mixtures of these two species, might furnish information

about their interactions. In particular, it might resolve whether "stick" or "slip" boundary conditions are applicable. If the former, one might expect rotational hindrance between the two species to be mutual, and that the reorientational behaviour of each species should respond in the same way to dilution with the other species. If the latter, the presence of a CCl_4 molecule might offer steric hindrance to the reorientation of a neighbouring C_6H_6 molecule, while reorientation of the more spherical CCl_4 molecule might proceed, indifferent of the presence of a C_6H_6 molecule.

Finally, a theoretical modification of the hydrodynamic model under "slip" boundary conditions, possibly via molecular dynamics calculations, would provide an opportunity for further interpretation of the present results.

References:

1. E. N. Ivanov, Sov. Phys. JETP 18, 1041 (1964).
2. F. J. Bartoli and T. A. Litovitz, J. Chem. Phys. 56, 404 (1972).

APPENDIX

THE LINEWIDTH ANALYSIS PROGRAM

```
          C      LEAST-SQUARES DETERMINATION OF BEST-FIT PARAMETER VALUES
          C      FOR DISTRIBUTIONS DESCRIBING LINE PROFILES
          C      DECONVOLUTION CAN BE PERFORMED IN CONJUNCTION WITH FITTING PROCEDURE
          C
0001             COMMON B(10,10),P(10),T(10),F(500),DP(10,500)
0002             REAL EST(10),TOL(10),W(400),E(400),D(10),S(100),TEST(10)
0003             DIMENSION KOUNT(400),KP(400),BR(10,10),DT(10)
0004             DIMENSION KS(100)
0005             READ (5,216) NOFITS
0006             DO 13 NODONE=1,NOFITS
0007             READ (5,201) MODE,NPAR,NSLIT,NMAX,NEDGE,DARK
0008             READ (5,203)  (KS(I),I=1,NSLIT)
0009             SUM = 0.
0010             DO 31 I = 1,NSLIT
0011          31 SUM = SUM + KS(I)
0012             DO 32 I=1,NSLIT
0013          32 S(I) = FLOAT(KS(I))/SUM
0014             READ (5,202) (EST(I),I=1,NPAR)
0015             DO 100 I=1,NPAR
0016             TOL(I) = 5. * EST(I)
0017         100 TEST(I) = .00001 * EST(I)
0018             READ (5,203) (KOUNT(I),I=1,NMAX)
          C
          C      INPUT PARTICULARS:
          C         'NOFITS' IS NO. OF SETS OF DATA TO BE PROCESSED
          C         (MODE=1) INVOKES OPTION TO CORRECT FOR STRAY LIGHT;
          C            (MODE=0) BYPASSES SAME
          C         'NPAR' IS NO. OF PARAMETERS TO BE OPTIMISED
          C         'NSLIT' IS NO. OF CHANNELS SPANNED BY SLIT FUNCTION
          C         'NMAX' IS NO. OF CHANNELS SCANNED IN DATA
          C         'NEDGE' IS NO. OF ADDITIONAL CHANNELS OF STRAY LIGHT DATA ON EACH
          C            SIDE OF 'KOUNT' DATA FIELD (ZERO WHEN MODE=0)
          C         'DARK' IS EXPECTED DARK COUNT IN EACH CHANNEL
          C            (NON-ZERO IF DARK COUNT IS TO BE SUBTRACTED ARBITRARILY)
          C         'SLIT(I)' IS VALUE OF NORMALISED SLIT FUNCTION IN I'TH CHANNEL
          C         'EST(I)' IS INITIAL ESTIMATE OF THE I'TH PARAMETER
          C         'TOL(I)' IS TOLERANCE WITHIN WHICH THE I'TH PARAMETER IS
          C            CONSTRAINED TO VARY
          C         'TEST(I)' IS THE LARGEST INCREMENT IN THE I'TH PARAMETER THAT
          C            IS DEEMED TO INDICATE CONVERGENCE
          C         'KOUNT(I)' IS THE DATUM FOR THE I'TH CHANNEL
          C         'KP(I)' IS THE STRAY LIGHT DATUM FOR THE I'TH CHANNEL
          C            (APPLICABLE WHEN MODE =1)
          C
0019             N = (NSLIT + 1)/2
0020             NRAR = NPAR
0021             DO 14 I=1,NRAR
0022          14 P(I) = EST(I)
0023             SUM = 0.
0024             DO 1 I=1,NMAX
0025             W(I) = 1./(KOUNT(I)+DARK)
0026           1 SUM = SUM+KOUNT(I)
0027             SUM = SUM - NMAX*DARK
0028             IF (MODE.EQ.0) GO TO 101
0029             NQAR = NPAR-1
0030             NMAXP = NMAX + 2*NEDGE
0031             READ (5,203) (KP(I),I=1,NMAXP)
0032             P(NQAR) = P(NQAR) / SUM
0033             NPAR = NPAR-2
0034         101 NMAXP = NMAX + NSLIT
0035             DO 2 I=1,NMAX
0036           2 E(I) = (KOUNT(I)-DARK)/SUM
0037             ITER = 0
```

```
0038          KGO = 1
0039          KCUT = 0
0040          CHISQ = 0.
0041          WRITE (6,204)
0042          WRITE (6,205 ) ITER,(EST(I),I=1,NRAR)
0043        3 DO 4 I=1,NRAR
0044          T(I) = 0.
0045          DO 4 J=1,NRAR
0046        4 B(I,J) = 0.
0047          DO 5 I=2,NMAXP
0048        5 CALL EVAL(I,NPAR,N)
0049          IF (MODE.EQ.0) GO TO 92
0050          ISHIFT = P(NRAR)
0051          IF ((P(NRAR)).LT.0.) GO TO 90
0052          IA = ISHIFT+NEDGE+1
0053          GO TO 91
0054       90 IA = ISHIFT+NEDGE
0055       91 IB = IA-1
0056          IC = ISHIFT+NEDGE
0057       92 IF  (KGO.EQ.1) GO TO 102
0058          WRITE (6,218)
0059          WRITE (6,208) (S(I),I=1,NSLIT)
0060          N1 = N+1
0061          N2 = N+NMAX
0062          WRITE (6,211)
0063          WRITE (6,208) (F(I),I=N1,N2)
0064      102 CONTINUE
0065          DO 106 I=1,NMAX
0066          F(I) = 0.
0067          DO 103 J=1,NSLIT
0068          IJ = I + J
0069      103 F(I) = F(I) + S(J) * F(IJ)
0070          IF (MODE.EQ.0 )  GO TO 20
0071          ID = I+IA
0072          IE = I+IB
0073          IG = I+IC
0074          PSHIFT = KP(IG) + (P(NRAR)-ISHIFT)*(KP(ID)-KP(IE))
0075          F(I) = F(I) + P(NQAR)*PSHIFT
0076       20 DY = E(I) - F(I)
0077          GO TO (22,21),KGO
0078       21 CHISQ = CHISQ + W(I) * DY**2
0079       22 DO 104 K=1,NPAR
0080          D(K) = 0.
0081          DO 104 J = 1,NSLIT
0082          IJ = I + J
0083      104 D(K) = D(K) + S(J) * DP(K,IJ)
0084          IF (MODE.EQ.0) GO TO 23
0085          D(NQAR) = PSHIFT
0086          D(NRAR) = P(NQAR)*(KP(ID)-KP(IE))
0087       23 DO 105 K=1,NRAR
0088          T(K) = T(K) + W(I) * DY * D(K)
0089          DO 105 J=K,NRAR
0090      105 B(K,J) = B(K,J) + W(I) * D(J) * D(K)
0091      106 CONTINUE
0092          MA = NRAR-1
0093          DO 6 I=1,MA
0094          MB = I+1
0095          DO 6 J=MB,NRAR
0096        6 B(J,I) = B(I,J)
0097          IF (KGO.EQ.1) GO TO 108
0098          DO 107 I=1,NRAR
0099          DO 107 J=1,NRAR
0100      107 BR(I,J) = B(I,J)
```

```
0101        108 CONTINUE
0102            CALL SOLVE(NRAR,KCUT)
0103            IF (KCUT.EQ.1) GO TO 13
0104            DO 7 I=1,NRAR
0105          7 P(I) = P(I)+T(I)
0106            IF (MODE.EQ.0) GO TO 24
0107            P(NQAR) = SUM * P(NQAR)
0108         24 DO 15 I=1,NRAR
0109            IF (ABS(P(I)-EST(I)).LT.TOL(I)) GO TO 15
0110            P(I) = EST(I)
0111         15 CONTINUE
0112            ITER = ITER+1
0113            IF (KGO.EQ.2) GO TO 12
0114            WRITE (6,205) ITER,(P(I),I=1,NRAR)
0115            IF (MODE.EQ.0 ) GO TO 8
0116            P(NQAR) = P(NQAR)/SUM
0117          8 IF (ITER-39) 9,11,12
0118          9 DO 10 I=1,NRAR
0119            IF ((ABS(T(I))).GT.(TEST(I))) GO TO 3
0120         10 CONTINUE
0121            IF (MODE.EQ.0) GO TO 11
0122            T(NQAR) = SUM * T(NQAR)
0123            IF ((ABS(T(NQAR))).GT.(TEST(NQAR))) GO TO 3
0124         11 KGO = 2
0125            GO TO 3
0126         12 CHISQ = CHISQ*SUM*SUM/(FLOAT(NMAX-NRAR))
0127            DO 17 I=1,NRAR
0128            DO 16 J=1,NRAR
0129         16 T(J) = 0.
0130            T(I) = 1./SUM**2
0131            DO 109 J=1,NRAR
0132            DO 109 K=1,NRAR
0133        109 B(J,K) = BR(J,K)
0134            CALL SOLVE(NRAR,KCUT)
0135         17 DT(I) = SQRT(T(I))
0136            IF (MODE.EQ.0)  GO TO 18
0137            DT(NQAR) = SUM*DT(NQAR)
0138         18 CONTINUE
0139            WRITE (6,209)
0140            WRITE (6,208) (F(I),I=1,NMAX)
0141            WRITE (6,207)
0142            WRITE (6,208) (E(I),I=1,NMAX)
0143            WRITE (6,212)
0144            WRITE (6,213)
0145            WRITE (6,205) ITER,(P(I),I=1,NRAR)
0146            WRITE (6,215) (DT(I),I=1,NRAR)
0147            WRITE (6,206) CHISQ
0148            WRITE (6,214) SUM
0149         13 CONTINUE
0150            CALL EXIT
0151        201 FORMAT (5I3,F6.3)
0152        202 FORMAT (6F12.6)
0153        203 FORMAT (10I6)
0154        204 FORMAT (1H1,9X,14HNO. OF ITER'NS,9X,2HMU,11X,5HGAMMA,9X,
              1 3HAMP,10X,4HBKGD,11X,1HC,11X,5HSHIFT//)
0155        205 FORMAT (14X,I2,7X,7F14.7)
0156        206 FORMAT (//20X,5HCHISQ,F20.5)
0157        207 FORMAT ( //10X,21HOBSERVED DISTRIBUTION/)
0158        208 FORMAT (10F12.6)
0159        209 FORMAT (//10X,24HTHEORETICAL DISTRIBUTION/)
0160        210 FORMAT (5F10.8)
0161        211 FORMAT (///10X,33HFILTERED THEORETICAL DISTRIBUTION/)
0162        212 FORMAT (///20X,22HFINAL PARAMETER VALUES)
```

```
0163        213 FORMAT ( //,9X,14HNO. OF ITER'NS,9X,2HMU,11X,5HGAMMA,9X,
               1 3HAMP,10X,4HBKGD,11X,1HC,11X,5HSHIFT//)
0164        214 FORMAT (///9X,12HTOTAL COUNTS,F20.0)
0165        215 FORMAT ( //9X,11HSTD. ERRORS,3X,7F14.7)
0166        216 FORMAT (I3)
0167        218 FORMAT (///10X,20HINSTRUMENTAL PROFILE//)
0168            END
```



```
0001            SUBROUTINE SOLVE(K,KCUT)
0002            COMMON B(10,10),P(10),T(10),F(500),DP(10,500)
0003            DO 10 L=1,K
0004            DO 5 J=L,K
0005            IF ((ABS(B(J,L))).LT.1.0E-15) GO TO 5
0006            DO 13 I=L,K
0007            C = B(J,I)
0008            B(J,I) = B(L,I)
0009            B(L,I) = C
0010         13 CONTINUE
0011            C = T(J)
0012            T(J) = T(L)
0013            T(L) = C
0014            GO TO 6
0015          5 CONTINUE
0016            WRITE (6,30)
0017            KCUT = 1
0018            RETURN
0019          6 M = L+1
0020            IF (M.GT.K) GO TO 8
0021            DO 7 J=M,K
0022          7 B(L,J) = -B(L,J)/B(L,L)
0023          8 T(L) = T(L)/B(L,L)
0024            IF (M.GT.K) GO TO 11
0025            DO 9 I=M,K
0026            DO 9 J=M,K
0027          9 B(I,J) = B(I,J)+B(L,J)*B(I,L)
0028            DO 16 I=M,K
0029         16 T(I) = T(I)-B(I,L)*T(L)
0030         10 CONTINUE
0031         11 DO 20 L=2,K
0032            M = K-L+1
0033            MA = M+1
0034            DO 12 I=MA,K
0035         12 T(M) = T(M)+T(I)*B(M,I)
0036         20 CONTINUE
0037            RETURN
0038         30 FORMAT (//20X, 15HMATRIX SINGULAR)
0039            END
```

```
0001          SUBROUTINE EVAL(I,NPAR,N)
0002          COMMON B(10,10),P(10),T(10),F(500),DP(10,500)
0003          J = I-N
0004          PI = 3.14159265
0005          C1 = (J-P(1))**2+P(2)**2/4.
0006          CS1 = PI*C1**2
        C
        C        'F(I)' IS THE VALUE OF THE UNCONVOLUTED DISTRIBUTION FUNCTION,
        C           EVALUATED USING CURRENT PARAMETER ESTIMATES, CORRESPONDING
        C           TO THE VALUE 'J' (=I-N) OF THE INDEPENDENT VARIABLE
        C
0007          F(I) = P(2)*P(3)/(2.*PI*C1)+P(4)
        C
        C        'DP(K,I)' IS PARTIAL DERIV. OF UNCONVOLUTED DISTRIBUTION
        C           FUNCTION W.R.T. K'TH PARAMETER, CORRESPONDING TO THE
        C           VALUE 'J' OF THE INDEPENDENT VARIABLE
        C
0008          DP(1,I) = P(3)*P(2)*(J-P(1))/CS1
0009          DP(2,I) = P(3)*(C1-P(2)**2/2.)/(2.*CS1)
0010          DP(3,I) = P(2)/(2.*C1)
0011          DP(4,I) = 1.
0012          RETURN
0013          END
```